

23 **TITLE**

24 **Sediment delivery to sustain the Ganges-Brahmaputra delta under climate change and**
25 **anthropogenic impacts**

26

27 **AUTHOR LIST**

28 Jessica L. Raff ¹, Steven L. Goodbred, Jr. ¹, Jennifer L. Pickering ², Ryan S. Sincavage ³, John C.
29 Ayers ¹, Md. Saddam Hossain ², Carol A. Wilson ⁴, Chris Paola ⁵, Michael S. Steckler ⁶, Dhiman R.
30 Mondal ⁷, Jean-Louis Grimaud ⁸, Celine Jo Grall ^{6,9}, Kimberly G. Rogers ¹⁰, Kazi Matin Ahmed ¹¹,
31 Syed Humayun Akhter ¹², Brandee N. Carlson ¹³, Elizabeth A. Chamberlain ¹⁴, Meagan Dejter ¹,
32 Jonathan M. Gilligan ¹, Richard P. Hale ¹⁵, Mahfuzur R. Khan ¹¹, Md. Golam Muktadir ¹⁶, Md.
33 Munsur Rahman ¹⁷, Lauren A. Williams ¹

34

35 **CORRESPONDING AUTHORS**

36 Jessica L. Raff (jessica.l.raff@vanderbilt.edu) and Steven L. Goodbred, Jr.
37 (steven.goodbred@vanderbilt.edu),

38

39 **AFFILIATIONS**

40 ¹*Department of Earth and Environmental Sciences, Vanderbilt University, Nashville, Tennessee,*
41 *USA*

42 ²*Center for Applied Earth Science and Engineering Research, The University of Memphis,*
43 *Memphis, Tennessee, USA*

44 ³*Department of Geology, Radford University, Radford, Virginia, USA*

45 ⁴*Department of Geology and Geophysics, Louisiana State University, Baton Rouge, Louisiana,*
46 USA

⁴⁹ ⁶ Lamont-Doherty Earth Observatory, Columbia University, Palisades, New York, USA

50 ⁷ Haystack Observatory, Massachusetts Institute of Technology, Westford, Massachusetts, USA

⁵¹ ⁸Centre de Géosciences, PSL University/ MINES Paris, Fontainebleau, France

52 ⁹ CNRS - Littoral Environnement et Sociétés, La Rochelle University, La Rochelle, France

53 ¹⁰ Institute for Arctic and Alpine Research, University of Colorado, Boulder, Colorado, USA

54 ¹¹ Department of Geology, University of Dhaka, Dhaka, Bangladesh

⁵⁵ ¹² Bangladesh Open University, Board Bazar, Gazipur, Bangladesh

⁵⁶ ¹³ Department of Earth and Atmospheric Sciences, University of Houston, Houston, Texas, USA

⁵⁷ ¹⁴ Soil Geography and Landscape Group, Wageningen University, Wageningen, Netherlands

⁵⁸ ¹⁵ Department of Ocean & Earth Sciences, Old Dominion University, Norfolk, Virginia, USA

⁵⁹ ¹⁶ Department of Environmental Science, Bangladesh University of Professionals, Dhaka,

60 *Bangladesh*

⁶¹ ¹⁷ Institute of Water and Flood Management, Bangladesh University of Engineering and
⁶² Technology, Dhaka, Bangladesh

63

64 **ABSTRACT**

65 The principal nature-based solution for offsetting relative sea-level rise in the Ganges-

66 Brahmaputra delta is the unabated delivery, dispersal, and deposition of the rivers' ~1 billion-

67 tonne annual sediment load. Recent hydrological transport modeling suggests that
68 strengthening monsoon precipitation in the 21st century could increase this sediment delivery
69 34-60%; yet other studies demonstrate that sediment could decline 15-80% if planned dams
70 and river diversions are fully implemented. We validate these modeled ranges by developing a
71 comprehensive field-based sediment budget that quantifies the supply of Ganges-Brahmaputra
72 river sediment under varying Holocene climate conditions. Our data reveal natural responses in
73 sediment supply comparable to previously modeled results and suggest that increased
74 sediment delivery may be capable of offsetting accelerated sea-level rise. This prospect for a
75 naturally sustained Ganges-Brahmaputra delta presents possibilities beyond the dystopian
76 future often posed for this system, but the implementation of currently proposed dams and
77 diversions would preclude such opportunities.

78

79 INTRODUCTION

80 Only in the past few years have global assessments of river-delta response to accelerated sea-
81 level rise and declining sediment supply utilized datasets more complete ^{1,2} than the single
82 mean values often used in earlier studies ³⁻⁵. Most earlier assessments yield grave predictions
83 for the response of deltas to climate change and human-related impacts, and while those
84 concerns are not unfounded, they generally oversimplify complex system behaviors and can
85 thus mask potentially more positive delta scenarios ². One risk of such negative but simplified
86 assessments is to foster dystopian narratives that uphold engineering structures or
87 abandonment of vast areas of coastal land as the key responses to climate change, thereby

88 undermining local to regional efforts to maintain sediment supply and preserve land in these
89 low-lying landscapes^{3,6}.

90 A robust supply of clastic sediment is the principal nature-based resource for offsetting
91 relative sea-level rise in river deltas, yet better constraints and data availability on the delivery
92 and dispersal of sediment are needed⁷ to ensure that future delta scenarios accurately account
93 for both dynamic natural-system behavior⁸ and the continuing impacts of development and
94 land-use change. Furthermore, it is increasingly important that coupled human-natural
95 approaches be used to predict delta fate, because as many as 630 million people currently live
96 in regions that may be uninhabitable by 2100 due to relative sea-level rise (RSLR), flooding, and
97 inundation⁹. Recent global delta studies using highly resolved, spatially and temporally varying
98 data inputs indeed suggest that more deltas than generally recognized have been gaining land
99 and that deltas overall may be collectively more robust than previously thought^{2,10–12}.

100 These recognitions are important because the fate of river deltas and their growing
101 populations are closely tied to riverine sediment supply¹⁰, which has a direct effect on land
102 reclamation efforts, household migration decisions, and the ability to occupy marginal
103 (vulnerable) lands^{13–15}. For instance, the relocation of >20,000 Rohingya refugees to a newly
104 emergent tidal island in the Ganges-Brahmaputra river-mouth estuary is a vivid example
105 involving each of these issues^{16,17}. In fact, the Bangladesh Delta Plan 2100 proposes numerous
106 coastal barriers (i.e., cross-dams) to trap sediment in the same region and accelerate the
107 growth of new land for potential reclamation and human occupation¹⁸. The social, engineering,
108 and political challenges of relocating displaced communities to emergent lands

109 notwithstanding¹⁹, a pre-requisite for coastal land reclamation remains the uninhibited delivery
110 of Ganges-Brahmaputra river sediment and its effective dispersal across the coastal zone.

111 Among the world's river deltas, the Ganges-Brahmaputra system presents an important
112 example of deltaic response to climate change and sea-level rise due to its naturally large
113 sediment supply, (currently) limited upstream damming, and an immense basin population of
114 ~500 million people²⁰. The basin's hydrology, climate, and sediment transport are controlled by
115 the seasonal South Asian monsoon, the strength of which varies considerably over decadal to
116 millennial timescales^{21–23}. Indeed, both modeling and proxy records document large
117 fluctuations throughout the Holocene, with stronger monsoon circulation and greater
118 precipitation from the early to mid Holocene followed by a general monsoon weakening and
119 reduction of precipitation after ~6 ka (Figure 2A,B)^{24–30}. For the coming century, the most
120 recent IPCC AR5 and AR6 reports continue to predict increased and more variable monsoon
121 precipitation by 2100 under nearly all representative GHG concentration pathways (RCPs)^{31,32}.

122 Such increases may be comparable to periods of stronger monsoon earlier in the Holocene, and
123 thus provide a possible analog for future responses. In addition to the strengthening of
124 monsoon precipitation, regional warming may also enhance the melting of Himalayan glaciers
125 and further increase discharge and sediment loads for at least the coming decades or century
126^{33,34}.

127 Observation-based estimates for the supply of sediment currently delivered to the
128 Ganges-Brahmaputra delta range from <500 to >1,100 Mt/yr (Mt = Mega-tonnes or 10^6 metric
129 tonnes), representing considerable uncertainty and a critical knowledge gap for projecting delta
130 response to sea-level rise^{7,35–37}. Looking forward, recent modeling studies by Darby et al.

131 (2015)³⁸, Dunn et al. (2018)³⁹ and Higgins et al. (2018)³³ each consider future changes in
132 Ganges-Brahmaputra sediment supply and their potential consequences for the delta. Their
133 findings suggest that historically unprecedented levels of change in sediment supply from the
134 Ganges and Brahmaputra rivers are possible over the next 50–100 years, either through
135 reductions from damming and diversions (e.g., Higgins et al. 2018)³³, increases from
136 strengthened monsoon precipitation and higher river discharge (e.g., Darby et. al., 2015;
137 Fischer et al., 2017)^{7,38}, or a combination of these factors (Dunn et al. 2018; Tessler et al.,
138 2018)^{39,40}. The modeled changes, although large ($\pm 50\text{--}90\%$), are comparable to other Asian river
139 systems that have experienced major changes in sediment load over the past century^{41–43}.

140 Toward a validation of such modelled projections of future sediment delivery to the
141 Ganges-Brahmaputra, we present a highly resolved, mass-balanced sediment budget that: (a)
142 utilizes over 6,000 new field-based measurements from 500 locations (Figure 1) to provide (b)
143 ground-truthing for modeling studies and (c) a holistic view of river system connectivity from
144 the Himalayan source terrains to the Bengal deltaic continental margin^{44,45}. The budget is
145 derived from previously unpublished borehole data on the volume, mass, grain size, and
146 provenance of Holocene sediment stored in the Bengal basin, and are supplemented by a
147 compilation of additional data from over 15 other studies (Tables 1, 2, S1). In addition to greatly
148 improved spatiotemporal resolution, this new work is distinct from previous Ganges-
149 Brahmaputra mass budgets^{46,47} that lacked any information on the river source (i.e.,
150 provenance) or grain-size distribution of stored sediments. Both of these new data types yield
151 valuable results on total bedload contribution to the delta and the varying and asymmetric
152 delivery of sediment from the two main rivers in response to climate change. To our

153 knowledge, no mass balance of comparable detail and longevity exists for a major river delta,
154 thus providing an unparalleled perspective on natural-system response to climate change and
155 an opportunity to ground-truth modeled responses under future climate scenarios.

156 Here we explore the validity of future sediment-delivery projections by comparing them
157 with previous responses of the Ganges-Brahmaputra sediment-load to Holocene climate
158 change and monsoon strength. To do so we use the new sediment database to carefully
159 quantify the mass and grain-size distribution (caliber) of sediment sequestered to the delta and
160 how that mass was distributed and stored to build the delta through major changes in climate
161 and sea level. Finally, we compare the reconstructions of sediment delivery and storage with
162 the sediment demands that will be required for the delta to offset projected increases in sea-
163 level rise for the coming century.

164

165 RESULTS AND DISCUSSION

166 Total Delta Sediment Composition

167 Reconstructed sediment storage rates from the stratigraphic record represent minimum total
168 riverine sediment loads (bedload and suspended load) delivered to the Ganges-Brahmaputra
169 delta. Unless otherwise noted, sediment delivery will be used to refer to sediment loads
170 reconstructed from stored Holocene sediments. The total mass of sediment stored in the
171 Ganges-Brahmaputra basin over the Holocene (12–0 ka) is $>1.2 \times 10^7$ Mt (Table 1), which
172 averages to a minimum mean delivery rate of ~1000 Mt/yr and is comparable to the oft-cited
173 modern load of ~1100 Mt/yr. The grain size of sediment stored in the delta is approximately
174 equally apportioned across muds (<62.5 μm – 30%), very fine to fine sand (62.5–250 μm – 39%),

175 and medium to coarse sand (250–1000 µm – 31%) (Table 1). For this study, we conservatively
176 classify sediments <250 µm (muds to fine sand) as suspended load and larger particles 250–
177 1000 µm as bedload ^{48,49}. These delineations result in Holocene delta deposits comprising ~70%
178 suspended load and 30% bedload sediments, considerably exceeding not only the 10% bedload
179 transport rate often presented in the literature where even high estimates are typically placed
180 at 20% ^{49–52}. The significance is that much of the long-term construction of the delta has been
181 through the aggradation of bedload sand, which is highly susceptible to upstream trapping in
182 reservoirs and thus an important consideration for future management of the delta ⁴¹.
183 Moreover, the bedload plays a disproportionate role in the growth of bars and other locally
184 elevated river topography upon which many village communities are sited.

185

186 **Variable Holocene Sediment Storage**

187 Despite similarity between the average modern and Holocene rates for sediment reaching the
188 delta, sediment delivery over millennial timescales varies by >200% from lowest delivery rates
189 of 850 Mt/yr through the mid-late Holocene (6–0 ka) up to maximum delivery rates in the early
190 Holocene of 1200 Mt/yr (8–6 ka) to 2000 Mt/yr (10–8 ka) (Table 1; Figure 2). Fluvial sediment
191 began aggrading in the Bengal basin beginning ~12 ka at a rate of ~820 Mt/yr (12–10 ka), but
192 delivery increased to at least 2000 Mt/yr (double the modern load) during the period of
193 strongest monsoon from 10–8 ka. These results confirm previous findings⁴⁷ that the Ganges and
194 Brahmaputra rivers carried a sediment load at least twice as large as the modern for over two
195 millennia. This large supply supported aggradation on the delta sufficient to offset very high
196 rates of sea-level rise that averaged >1 cm/yr over this period. These high early Holocene rates

197 of sediment delivery and sea-level rise are comparable to those anticipated for the next century
198 based on the Darby et al.³⁸ modeling for sediment supply and IPCC projections for sea-level rise
199⁵³. These similarities between our paleo-reconstructions and the modeled futures of other
200 studies highlight a potential scenario of sediment supply whereby the delta may be able to
201 maintain itself against increases in sea-level rise over the next century.

202 Emphasizing that our budget reconstructions represent minimum supply rates, the
203 portions of sediment load that bypassed the delta and transported to the Swatch of No Ground
204 canyon and deep-sea Bengal Fan^{54,55} are not included in the Holocene sediment delivery rates.
205 Such sediment bypass would have been greatest from 12–8 ka when the river channels were
206 constrained to their lowstand valleys and discharged directly to the canyon head. Simple
207 reconstructions of mud deposition in the Swatch of No Ground and active channel of the Bengal
208 Fan^{56–58} suggest that as much as another ~200 Mt/yr of sediment may have been delivered by
209 the rivers in the early Holocene. After 8 ka, though, most sediment delivered to the Bengal
210 margin was efficiently trapped in the Ganges-Brahmaputra delta and thus accounted for in our
211 sediment budget; this sequestration of sediment in the delta is well reflected by the abrupt
212 drop in sedimentation on the Bengal Fan after 9 ka, despite continued high river discharge^{56–58}.

213 In addition to variation in total mass delivered, the sediment loads between 12–10 ka
214 and 10–8 ka are considerably coarser than the Holocene average, comprising ~37% medium to
215 coarse sand that was presumably transported as bedload (Table 1). In contrast, the proportion
216 of med-coarse sand stored in the delta decreases to ~22% after 8 ka. Compared with modern
217 estimates, these Holocene values are considerably higher than the 10-20% bedload fraction
218 often assumed for the total Ganges-Brahmaputra sediment load^{49–52}, although one modern

219 study does cite a bedload fraction of ~35% for each river that is similar to our Holocene
220 fractions. Regardless of the exact value, our results emphasize that the importance of sand
221 delivery by these large, braided rivers for future delta stability should not be undervalued,
222 particularly in context of the massive mining of river sands occurring in the Ganges-
223 Brahmaputra and other rivers worldwide^{59,60} and the effective trapping of bedload by
224 upstream reservoirs⁶¹.

225

226 **Ganges and Brahmaputra Sediment Provenance**

227 Using bulk Sr concentration of stored sediments, which has been shown to be a reliable
228 indicator of river source in this system^{62–64} (Figure S1), we have quantified the fraction of
229 sediments delivered to the delta by the Ganges, Brahmaputra, and smaller local rivers (Table 2).
230 Results for the Holocene show that nearly 54% of sediments were sourced by the Brahmaputra,
231 ~30% by the Ganges, and the remaining ~14% by local rivers including the Tista River in
232 northwest Bangladesh and others draining the Indo-Burman fold belt and Shillong Massif to the
233 east (see Methods for further details). Both major rivers demonstrate considerable variability in
234 sediment delivery throughout the Holocene, but responses are most pronounced for the
235 Brahmaputra catchment (Table 2, Figure 2). Since 10 ka, the long-term averages for Ganges
236 sediment load ranges 308 to 426 Mt/yr, which is comparable to the variance in modern load
237 estimates of 300–450 Mt/yr^{37,65,66}. This suggests that Ganges discharge has been relatively
238 stable even with considerable regional climate variability, a finding that is consistent with the
239 similarly modest response projected by Darby et al. (2015) under future climate scenarios. Note
240 that the low Ganges value of 116 Mt/yr stored from 12–10 ka (Table 2) is likely an

241 underestimate due to sediment bypassing, as sedimentation on the Bengal fan remained high
242 at this time^{56,58}.

243 In contrast, sediment load for the Brahmaputra has been highly variable over the
244 Holocene, with a 4-fold range from a high of ~1100 Mt/yr at 10–8 ka to a low of ~370 Mt/yr
245 from 6–0 ka. Relative to the Brahmaputra's modern load of 500–650 Mt/yr, these values
246 represent a long-term doubling and halving over the Holocene, respectively, reflecting acute
247 response to monsoon strength and related sediment production and transport processes. As
248 for the Ganges, the magnitude of response for our Brahmaputra reconstructions is similar to
249 the projections made by Darby et al. (2015), lending confidence to their results of increased,
250 but differential, future sediment transport for each river. In particular, the differing response of
251 Ganges and Brahmaputra sediment load to climate change will remain highly relevant to
252 managing the delta, given that the largest sediment-source areas for the two rivers lie in India
253 and China, respectively.

254

255 **Response to monsoon variability**

256 The modeling of river discharge under future climate change suggests that increases in Ganges-
257 Brahmaputra sediment load of 34–60%³⁸ are possible, which would be a substantial increase in
258 sediment delivered to the delta and thus a potentially important buffer against accelerated
259 rates of sea-level rise. These modeled values are supported by our findings from the early
260 Holocene period (12–8 ka) of strengthened monsoon, when fluvial sediment loads were higher
261 for both river systems compared to periods of weaker monsoon from 8–0 ka. Over this full
262 range of monsoon conditions, the Brahmaputra sediment load varied from 377–1119 Mt/yr

263 (i.e., a ± 2 -fold difference from modern), whereas the Ganges varied only 308–426 Mt/yr (i.e., a
264 range comparable to modern estimates). Note we do not include here the low Ganges value of
265 116 Mt/yr for the 12–10 ka period due to presumed sediment bypassing at this low sea-level
266 stage.

267 Our sediment budget reconstructions are also consistent with the results of Darby et
268 al.³⁸ further suggesting that the Brahmaputra River catchment is considerably more sensitive to
269 changes in climate, and that during wetter periods it is the more dominant source of sediment
270 to the delta. Importantly, there is no overlap in methods between our paleo-reconstructions
271 and the forward-looking projections of Darby et al. (2015)³⁸, suggesting that the comparable
272 results provide a reasonable reflection of Ganges-Brahmaputra system dynamics. Among the
273 reasons for such an acute response from the Brahmaputra relative to the Ganges is the
274 catchment's proportionally smaller lowland area³⁸ that limits its capacity for sediment storage.
275 This reduced buffering capacity means that variations in sediment yield from the Brahmaputra
276 catchment reach the delta more quickly and with less attenuation than those from the Ganges
277 catchment⁴⁴. Another factor contributing to acute response of the Brahmaputra sediment
278 supply to climate is the catchment's large area of relatively arid and sparsely vegetated
279 highlands in Tibet, where modest changes in the water budget can drive much higher or lower
280 erosion rates⁶⁷. Moreover, recent (2003–2008) loss of glacial elevation in the Himalayan
281 catchments⁶⁸ introduces glacial melt as another source of increased discharge and sediment
282 delivery, although persistence of this contribution may wane beyond 2100 as ice extent
283 contracts³.

284 In contrast to the Brahmaputra, the Ganges catchment lies at the center of the South
285 Asian monsoon system with robust precipitation and vegetation across the Himalayan front
286 range, which is where most sediment and water discharge are generated. The Ganges also
287 hosts a vast foreland filled by alluvial mega-fans that are capable of storing sediment; however,
288 their ability to buffer short-term changes in sediment supply is limited because many fan
289 channels in the Ganges basin are incised and decoupled from the adjacent plains, or are
290 otherwise heavily embanked like the Kosi River fan⁶⁹, causing greater downstream bypass of
291 sediment^{52,70}. Indeed, during the early Holocene when the monsoon was strong, the Ganges
292 system incised and remobilized megafan sediments that had aggraded in the early post-glacial
293 period^{70–72}. These phenomena in the Ganges catchment support results from models indicating
294 that variable water supply (e.g., due to fluctuations in monsoon strength) can cause periods of
295 aggradation when water flux decreases and periods of incision when water flux increases⁷³.
296 Overall, the Ganges fan systems serve to buffer variance in sediment supply as compared with
297 the Brahmaputra that has proportionally less lowland storage area, which is well reflected in
298 both our Holocene reconstructions and the Darby et al.³⁸ scenarios for the next century.

299 Given interest in the potential increase in sediment load under future climate scenarios,
300 it is important to also consider the timescales at which sediment stored in the upper catchment
301 may be remobilized from hillslope, valley, and floodplain settings and delivered to the delta.
302 Our paleo-reconstructions do not provide great precision on those timescales, but evidence
303 from both the Ganges-Brahmaputra and the Indus delta systems show that changes in the
304 supply of riverine sediment load respond to monsoon precipitation at timescales less than the
305 sub-millennial resolution of radiocarbon-dated stratigraphic sections^{47,74}. Such short response

306 times would indeed be consistent with hydrologically driven changes in transport and an
307 abundance of available sediment (i.e., a transport limited system)⁷³. Indeed ~95% of the
308 Ganges-Brahmaputra sediment load is delivered during the summer monsoon and resulting
309 period of high river discharge (May–October). In this context, more precipitation over the
310 catchment readily remobilizes abundant sediment stored as hillslope regolith and alluvial
311 deposits in the upper catchment. Modern examples also appear to confirm rapid sediment
312 transfer from upland source areas to the Bengal margin, perhaps best exemplified by the
313 decadal-scale transport and delivery of Brahmaputra bedload introduced by 100s of landslides
314 generated in the major 1950 Assam earthquake (M 8.6)^{75,76}. Similarly, HydroTrend, the climate-
315 driven hydrological water balance and transport model used by Darby et al. (2015)³⁸ to consider
316 future basin response to increased precipitation, does not suggest any significant lag time for
317 the delivery of Ganges-Brahmaputra sediment to the delta⁷⁷.

318

319 **Increasing sediment supply to support increasing sediment need**

320 To better understand the implications of varying sediment load and rates of sea-level
321 rise on delta sustainability, we have produced mass balance estimates under a variety of past,
322 present, and future scenarios (Figures 3 and 4). The Δ Mass rates (Mt/yr) represent the annual
323 excess (>0) or deficit (<0) supply of sediment for each scenario, and the $f_{(supply)}$ is the fractional
324 excess or deficit of delivered sediment specifically for the medium-demand scenario. Results
325 show an excess of sediment delivery under most natural conditions during the Holocene and
326 modern, even during periods of rapid sea-level rise comparable to the rates anticipated for the
327 coming century (5 to 12.5 mm/yr) (Figures 3 and 4). The modern mass delivery also readily

328 meets demand using the most often reported sediment load value of 1100 Mt/yr, but the delta
329 would be facing a measurable deficit if the occasionally cited value of 700 Mt/yr were correct
330^{35–37,65}. Given the Ganges-Brahmaputra delta's persistent growth in land area over the last few
331 decades and centuries^{78–80}, the higher value of 1100 Mt/yr appears to be more accurate. For
332 the future, unabated sediment delivery in the 2050 and 2100 climate-only scenarios yield a
333 $f_{(supply)}$ ranging from a slight to moderate deficits of 7–20%, meaning that erosion rates and land
334 loss may be correspondingly slow and provide valuable time for mitigation strategies to be
335 implemented. These mass balance results (Figure 3) are consistent with persistent growth of
336 the delta from Holocene to modern and are not simply optimistic calculations. Rather, these
337 reconstructions and future scenarios (Figures 3 and 4) emphasize natural resilience of the
338 Ganges-Brahmaputra delta linked to the region's robust monsoon precipitation and high
339 sediment yield from the tectonically active Himalayan Mountains.

340 Evidence of a robust and resilient Ganges-Brahmaputra delta has received less attention
341 than scenarios considering a heavily engineered future, where major sediment reductions and
342 high rates of land loss are likely – yet both outcomes are plausible, and the eventual pathway is
343 more contingent on the decisions of policy makers than on climate change. Indeed, our mass
344 balance estimates (Figure 3) show massive sediment deficits of more than 100% to over 2000%
345 under all future scenarios that consider widespread dam construction and water diversions^{38–40}.
346 These futures are the ones that will more aptly compare the Ganges-Brahmaputra delta with
347 the catastrophic land loss already occurring in the Mississippi, Nile, Indus, Mekong, and other
348 deltas fed by heavily dammed rivers^{5,81,82}. Thus, the Ganges-Brahmaputra delta is not doomed

349 to drown under climate change – it is doomed to drown under scenarios of anthropogenic
350 reductions in the sediment delivery needed to sustain the delta⁸³.

351 Many damming and diversion plans for the Ganges and Brahmaputra rivers have been
352 developed but not yet widely implemented³³, thus presenting a window of opportunity to
353 better steward the delta future. A major risk of not acknowledging the Ganges-Brahmaputra
354 system's intrinsically robust sediment supply and potential resilience against rising sea level is
355 that environmental managers will otherwise plan for the dystopian future of a drowning
356 landscape and the development of policies that steer toward this anticipated outcome of ruin
357^{6,84}.

358 Although the potential for considerably enhanced sediment delivery to the Ganges-
359 Brahmaputra delta exists, it alone would still be insufficient to sustain the system. Rather,
360 delivered sediment must also be allowed to freely disperse to regions of the delta where it is
361 needed to offset subsidence and rising sea level. Within the delta itself, widespread
362 embankments in the tidally influenced coastal zone already limit such sediment delivery to
363 poldered islands^{83,85} and have exacerbated local sea-level rise^{86,87}. Potentially sustainable
364 efforts to manage sediment accretion in these embanked polders are underway but still face
365 implementation challenges^{10,88,89}.

366 In contrast, in natural areas of the delta such as the Sundarbans mangrove forest, a
367 protected UNESCO World Heritage site, and the Ganges-Brahmaputra's Meghna rivermouth
368 estuary, unhindered sedimentation is rapid and is readily keeping pace with effective sea-level
369 rise (0.5-1.5 cm/yr)^{83,90,91}. In fact, in the rivermouth estuary, low barriers (i.e., cross dams) built
370 across shallow waterways have been effective at trapping sediment and rapidly converting

371 open water to emergent intertidal and supratidal lands. Such land reclamation projects are a
372 key part of Bangladesh's plans for mitigating the effects of sea-level rise¹⁸, but the success will
373 require the continued uninhibited delivery and dispersal of sediment. Even under scenarios of
374 enhanced sediment delivery, maintaining these natural morphodynamic processes will remain
375 an essential ingredient for long-term sustainability of the delta, which cannot be fully managed
376 or hardened given its size, complexity, and large mass and energy inputs^{8,92}.

377

378 **Anthropogenic threats to future sediment delivery**

379 Despite projected increases under a strengthened monsoon, anthropogenic factors may
380 yet dominate the system-scale responses and drive sediment loads to be considerably lower.
381 Specifically, plans across South Asia for hydropower development and interbasinal watershed
382 management portend major reservoir construction and water diversions in the coming century
383^{33,93}. Modeling of the impact of these activities on the river basins suggests moderate (30%) to
384 extreme (88%) decreases in sediment discharge under a range of plausible river-management
385 scenarios^{33,39} (Figure 3). Existing studies focus on the impact of India's National River Linking
386 Project (NRLP) and hydropower projects in Nepal, both of which disproportionately affect the
387 Ganges river system^{33,39}. No study has yet assessed the potential impact of China's proposed
388 Motuo hydropower project that would be a run-of-the-river dam of the Yarlung Tsangpo^{93,94},
389 which is a primary water and sediment source estimated to supply 50% of the Brahmaputra's
390 downstream sediment load.

391 Uncertainty in the Ganges-Brahmaputra delta sediment budget hinders the ability to
392 create sustainable development plans⁷ and makes it possible for upstream decision-makers to

393 justify continued dam construction and water diversions^{95–98} at the expense of downstream
394 sediment supply to the delta^{95,99}. Reduced sediment supply will threaten delta stability,
395 particularly if loads decrease below those needed to maintain the delta surface above sea level
396^{88,90}. In other mega-deltas like the Mekong and Mississippi, reduced sediment loads from
397 damming and sand extraction have already led to increased saltwater intrusion, decreased soil
398 fertility, loss of land area with rising sea level, and elevation deficits that increase susceptibility
399 to flooding and storm surges^{5,81,82}.

400 Amidst typically negative risk assessments of the Ganges-Brahmaputra delta, it is rarely
401 acknowledged that the system has persistently gained several km²/yr of land-surface area for at
402 least the last several centuries, a pattern that continues today without any sign of waning^{83,92}.
403 With the next century of climate change, models indicate that the delivery of sediment to the
404 delta will not only persist but likely increase considerably, with the potential to offset
405 accelerating rates of sea-level rise^{7,38}. Such projections are consistent with the Holocene
406 sediment reconstructions presented here (Figures 2 and 3), and these results collectively
407 suggest that the Ganges-Brahmaputra delta may be among the world's most naturally resilient
408 large coastal systems.

409 The magnitudes of sediment delivery suggested by our field-based reconstructions and
410 the modeled natural scenarios are very similar, suggesting that the results are reasonably
411 robust; however, even if future increases in sediment load are less than suggested here, a key
412 point is that any increase in sediment supply has the potential to mitigate the impacts of sea-
413 level rise and delay delta drowning. Realizing this potential, though, not only depends on
414 downstream policy decisions that affect the distribution and fate of this sediment in the delta,

415 but also the affects of upstream sediment diversions or retention that threaten the ability of
416 even the wisest downstream policies to mitigate coastal land loss. With global warming and
417 sea-level rise baked into the climate system for centuries, any factors such as increased
418 sediment delivery that can delay or reduce impacts may be critically important for effective and
419 manageable human responses.

420

421 **Importance of perception to delta futures**

422 Increased sediment delivery under a strengthened monsoon supports the possibility for
423 a more favorable Ganges-Brahmaputra delta outcome under a majority of future climate
424 scenarios. These natural-system responses to climate variability support conclusions from
425 future model scenarios for the coming century^{38,100} and modern field-based studies^{83,90} that
426 the delta is not inherently doomed to drown. Instead, proper management of sediment
427 resources, particularly within at-risk coastal regions^{85,88}, may provide security for coastal
428 populations and livelihoods often presented as unviable under future climate scenarios^{6,13,84,101}.
429 However, the persistence of a doomed-to-drown narrative for Bangladesh may perpetuate
430 dystopian views in which particular regions of the delta or livelihoods are considered
431 unsustainable and thus become subject to maladaptive policies⁸⁴ and may remove attention
432 from the importance of international agreements to coordinate the transport of sediment
433 across national boundaries. Such perceived threats shift the focus of mitigation projects toward
434 the strengthening or expanding of hard infrastructure, approaches that have already disrupted
435 sedimentation processes and undermine the delta's natural resilience to sea-level rise⁸. The
436 resulting impacts may exacerbate the displacement of households and increase migration away

437 from these supposedly unsustainable coastal locations⁶. Although hard-engineering responses
438 may continue to be part of a sensible coastal management plan, adopting them under threat of
439 a dystopian future may steer policies away from more nature-based solutions and other
440 sustainable development policies that would bolster long-term stability of the coastal zone
441 through the effective management of sediment delivery and dispersal.

442 Upstream of the delta, though, a key concern is how the supply of sediment reaching
443 the delta will be impacted by anthropogenic activities in the catchment basin. In other words,
444 any natural increase in sediment delivery resulting from increased monsoon precipitation^{38,100}
445 will compete with anthropogenic decreases caused by the construction of proposed dams and
446 water diversions upstream of the delta^{33,39,88} (Figures 3 and 4). Managing these different
447 factors in order to maintain a sustainable delta requires continued diplomatic and scientific
448 focus on the transboundary transport of sediment—focus that is difficult to maintain if a
449 dystopian narrative dominates public discourse. In all, the work presented here and by others
450^{2,83} offers the possibility for a more optimistic future that is often absent in the literature and
451 media coverage of the Ganges-Brahmaputra delta. The emerging narrative on fate of the delta
452 shifts somewhat away from climate change and more toward the sustainable management of
453 water and sediment resources, both in the upstream catchment and across the delta itself.
454 While there are still significant issues with regard to the uneven distribution of sediment across
455 the delta¹⁰², the total available sediment could be sufficient for continued sustainability of the
456 delta system as a whole. The caveat is that the delta may only be more resilient to climate
457 change in the absence of major dam construction and water diversions upstream of the delta
458 and major disruptions to the effective delivery and dispersal of sediment within the delta.

459

460 **METHODS**

461 **Data source**

462 The sediment budget is produced from a largely unpublished dataset of sediment grain-size and
463 geochemistry measured on 6,100 sediment samples from 455 boreholes collected by the
464 authors and colleagues between 2011-2021. The boreholes have a maximum depth of 95 m and
465 were collected in 23 transects across the delta. The stratigraphy for about half of these cores
466 (~200) has been published in five previous papers ^{103–107}, the radiocarbon ages are published in
467 Grall et al. (2020), and local grain-size and mass-balance for one sub-basin of the delta
468 published in Sincavage et al. (2019). These data are supplemented by widespread core and
469 seismic data previously published by Ahmed et al. (2010), Bangladesh Agriculture Development
470 Corporation (1992), Shamsudduha et al. (2008), Pate et al. (2009), Department of Public Health
471 Engineering and Japanese International Cooperation Agency (JICA) (2006), JICA (1976), Ghosal
472 et al. (2015), Hait et al. (1996), Hoque et al. (2012), Hoque et al. (2014), Khan & Islam (2008),
473 Michels et al. (1998), Palamenghi et al. (2011), and Sarkar et al. (2009) ^{108–122}. These
474 supplemental data extend across the entire Bengal Basin, including the continental shelf and
475 West Bengal, India where we do not have samples. The complete compilation of data from
476 these sources adds 3,720 sites to the more detailed results from our 455 cores.

477

478 **Field and laboratory methods**

479 Sediment samples for the cores in this study were collected at 1.5-m depth intervals and
480 photographed, described, and packaged in the field ^{104–106}. In the lab, every third sample with

481 depth as well as samples at sedimentologic contacts were analyzed for grain-size distribution
482 using a Malvern Mastersizer 2000E particle size analyzer at $\frac{1}{4}\varphi$ intervals from clays (0.49 μm)
483 to coarse sands (1000 μm). Samples were also analyzed for bulk geochemistry by X-ray
484 fluorescence using a portable Thermoscientific Niton XL3 Analyzer (pXRF), which returns
485 information on composition of both major and trace elements in the sediments. Strontium
486 concentrations from the XRF results are used to document sediment provenance following
487 published methods⁶², effectively distinguishing sediment deposited by the Ganges,
488 Brahmaputra, mixed Ganges-Brahmaputra, or other local river sources^{62–64} (Figure S1).
489 Sediments having higher bulk Sr values >130 ppm are derived from the Brahmaputra basin,
490 which drains mafic batholiths along the Tsangpo suture zone, compared with lower bulk Sr
491 values < 110 ppm for the Ganges (in central and western areas of the delta) or local sediment
492 sources in the north (Tista River), northeast (Shillong Massif), and east (Indo-Burman Fold Belt).
493 Of the 6100 samples analyzed to date for grain size and geochemistry, over 4,000 are Holocene-
494 aged and included in this study.

495

496 **Mapping**

497 Mapping of Holocene Ganges-Brahmaputra delta deposits was performed using ArcGIS. The
498 Holocene-Pleistocene boundary depth was identified using sediment grain size, color as a proxy
499 for oxidation state, and radiocarbon data from the aggregated dataset^{103–106,114,123,124} and
500 supplemented with depth data from cores, wells, and seismic data in reports and previously
501 published studies^{108–121}. Simple co-kriging was used to create an interpolated prediction
502 surface of the depth to the Pleistocene boundary from both the hand drawn contours and

503 depth information from >950 core sites and hundreds of kilometers of seismic lines from many
504 studies^{108–121}. To synthesize the data from these 6000+ samples and to control for variance
505 related to regional tectonics and structure, antecedent Pleistocene topography, and the
506 backwater and coastal transition, we partitioned the delta into 9 physiographic and
507 depositional regions based on similarities in processes and inputs (see FigURS2). Several of
508 these regions are parsed further into sub-regions, largely based on the core-data distribution,
509 to increase the sediment budget resolution and to account for downstream fining and fluvial
510 depositional processes. The main provinces include the Jamuna valley, Ganges valley, Sylhet
511 basin, Meghna valley, Fold Belt, Madhupur Terrace, West Bengal, Interfluve, and Offshore. We
512 then regroup these sub-regions into valleys (Jamuna valley, Ganges valley, Meghna valley),
513 interfluves (Madhupur Terrace, Paleo-interfluve, Fold Belt, West Bengal), and basins (Offshore,
514 Sylhet Basin). To better understand the subsurface stratigraphy, we calculated the grain-size
515 distribution of all samples by 5-m depth bins within spatiotemporal units and then multiplied by
516 the total sediment mass in that unit to yield the sediment-mass grain-size distribution by depth
517 for each region ($n=251$; see supplemental materials).

518 Due to spatially varying subsidence rates and temporally changing eustatic sea-level rise
519 that control accommodation in the delta, simple depth conversions do not correlate well with
520 age of the deposits. In other words, establishing well-defined time horizons from radiocarbon
521 ages is complicated by instantaneous variations in delta surface topography. However,
522 averaged over longer periods typical of channel avulsion and migration (i.e., 1000–2000 years),
523^{62,105,125} a stable or growing delta system must infill accommodation generated. Therefore, the
524 potential mass of stored sediment at any given interval will be a function of the volume created

525 by subsidence and sea-level rise. Thus, the Holocene unit has been partitioned into Time-
526 Equivalent depositional units (TEQ) based on regional subsidence patterns derived from a large
527 radiocarbon database ($n > 200$) in Grall et al. (2018)¹²³ and combined with eustatic sea-level
528 reconstructions from Lambeck et al. (2014)¹²⁶. These relative sea-level rise controls were used
529 to map the base-level and delta surface at 6 ka, 8 ka, 10 ka, and 12 ka. The resulting surfaces
530 were spliced in GIS to form TEQ units that correspond to accommodation generated during the
531 periods 6–0 ka, 6–8 ka, 8–10 ka, 10–12 ka. To calculate the delta surface over which
532 sediments were deposited and the volume of material stored during each TEQ, we subtracted
533 the interpolated Holocene surface from the effective subsidence (land subsidence and sea-level
534 rise) over those years in ArcGIS (Figure S2, Table S1). The volume of each TEQ was multiplied by
535 a mean bulk density based on field measurements to derive the mass of sediment stored on the
536 delta during each TEQ. The bulk densities used range from 1.3 g/cm³ in the shallow units to 1.8
537 g/cm³ in the deepest units, and a lower value of 1.1 g/cm³ for muddy coastal and shelf units. To
538 calculate the grain-size distribution of each sediment package, we isolated the samples from
539 each core contained within the TEQ, calculated the average grain-size distribution, and
540 interpolated the grain-size distribution to the total mass of the material in each TEQ.

541

542 **Offshore and West Bengal delta regions**

543 For the offshore and West Bengal physiographic regions where we have not collected cores, we
544 base the budget calculations on published studies. For the offshore, growth of the subaqueous
545 delta began after ~8 ka and the stored sediment mass determined from seismic and core data
546^{56,127}. Our budget calculations proportionally distribute 75% of this offshore delta sediment to

547 the 6–0 ka interval and 25% to the 8–6 ka interval. The source of offshore sediment was
548 partitioned between Brahmaputra (~60%) and Ganges (~40%) based on Sr measurements of
549 shelf sediment by Garzanti et al. (2019)¹²⁸ and Lupker et al. (2013)¹²⁹. The grain-size
550 distribution of sediments stored in West Bengal is taken from previously published data in
551 Stanley & Hait (2000)¹³⁰, who measured the mud:sand ratio to be ~70:30 in a series of
552 Holocene-scale cores (<50 m). The average Holocene thickness of sediments in their cores was
553 25 m with a maximum thickness of ~45 m. Although kriging analyses show the maximum
554 predicted thickness of Holocene sediments in West Bengal to be ~70 m, >90% of the total
555 sediment package is stored in the upper 45 m, so the data from Stanley & Hait (2000) can be
556 used. For comparison, our data from the Ganges-Brahmaputra interfluve east of the Ganges
557 valley and just opposite the West Bengal region is a comparable ~63% mud and ~37% sand.
558 Since this grain-size distribution aligns well with measurements from West Bengal¹³⁰, we apply
559 the same distribution for sediment stored in that region.

560

561 **Sediment surplus and deficit calculations**

562 A simple mass-balance model compares the mass aggradation needed to offset relative
563 sea-level rise (RSLR) for the Ganges-Brahmaputra delta with reconstructed sediment delivery
564 rates (Figure 3). The upper delta extends from the delta apex to the slope break at the fluvial-
565 to tide-influenced transition (Figure S3), the lower delta from the tidal transition at the slope
566 break to the coast, and the marine delta from the coast to base of the subaqueous delta
567 foresets. We apply mean subsidence rates and mean eustatic sea level to each of these regions

568 using a bulk density of 1.5 t/m³ typical of the upper 20 m of sediment. Additional details on
569 calculation steps are provided in Figure 3.

570

571 **Data availability**

572 The sediment data generated in this study are provided in the Supplementary Information file.

573

574 **REFERENCES**

- 575 1. Caldwell, R. L. *et al.* A global delta dataset and the environmental variables that predict
576 delta formation on marine coastlines. *Earth Surf. Dyn.* **7**, 773–787 (2019).
- 577 2. Nienhuis, J. H. *et al.* Global-scale human impact on delta morphology has led to net land
578 area gain. *Nature* **577**, 514–518 (2020).
- 579 3. Tessler, Z. D. *et al.* Profiling risk and sustainability in coastal deltas of the world. *Science*
580 (*80-*). **349**, 638–643 (2015).
- 581 4. Renaud, F. G. *et al.* Tipping from the Holocene to the Anthropocene: How threatened are
582 major world deltas? *Curr. Opin. Environ. Sustain.* **5**, 644–654 (2013).
- 583 5. Syvitski, J. P. M. *et al.* Sinking deltas due to human activities. *Nat. Geosci.* **2**, 681–686
584 (2009).
- 585 6. Paprocki, K. On viability: Climate change and the science of possible futures. *Glob.*
586 *Environ. Chang.* **73**, 102487 (2022).
- 587 7. Fischer, S., Pietroń, J., Bring, A., Thorslund, J. & Jarsjö, J. Present to future sediment
588 transport of the Brahmaputra River: reducing uncertainty in predictions and
589 management. *Reg. Environ. Chang.* **17**, 515–526 (2017).

- 590 8. Passalacqua, P., Giosan, L., Goodbred, S. & Overeem, I. Stable ≠ Sustainable: Delta
591 dynamics versus the human need for stability. *Earth's Futur.* **9**, e2021EF002121 (2021).
- 592 9. Kulp, S. A. & Strauss, B. H. New elevation data triple estimates of global vulnerability to
593 sea-level rise and coastal flooding. *Nat. Commun.* **10**, (2019).
- 594 10. Cox, J. R. *et al.* A global synthesis of the effectiveness of sedimentation-enhancing
595 strategies for river deltas and estuaries. *Glob. Planet. Change* 103796 (2022).
596 doi:10.1016/J.GLOPLACHA.2022.103796
- 597 11. Nienhuis, J. H., Hoitink, A. J. F. T. & Törnqvist, T. E. Future Change to Tide-Influenced
598 Deltas. *Geophys. Res. Lett.* **45**, 3499–3507 (2018).
- 599 12. Leuven, J. R. F. W., Pierik, H. J., van der Vegt, M., Bouma, T. J. & Kleinhans, M. G. Sea-
600 level-rise-induced threats depend on the size of tide-influenced estuaries worldwide.
601 *Nat. Clim. Chang.* **9**, 986–992 (2019).
- 602 13. Gain, A. K. *et al.* Overcoming challenges for implementing nature-based solutions in
603 deltaic environments: Insights from the Ganges-Brahmaputra delta in Bangladesh.
604 *Environ. Res. Lett.* **17**, (2022).
- 605 14. Mallick, B., Rogers, K. G. & Sultana, Z. In harm's way: Non-migration decisions of people
606 at risk of slow-onset coastal hazards in Bangladesh. *Ambio* **51**, 114–134 (2022).
- 607 15. Khatun, F. *et al.* Environmental non-migration as adaptation in hazard-prone areas:
608 Evidence from coastal Bangladesh. *Glob. Environ. Chang.* **77**, 102610 (2022).
- 609 16. Islam, M. R., Islam, M. T., Alam, M. S., Hussain, M. & Haque, M. M. Is Bhasan Char Island,
610 Noakhali district in Bangladesh a sustainable place for the relocated Rohingya displaced
611 people? An empirical study. *SN Soc. Sci.* **1**, 1–24 (2021).

- 612 17. Islam, M. D. & Siddika, A. Implications of the Rohingya Relocation from Cox's Bazar to
613 Bhasan Char, Bangladesh. *Int. Migr. Rev.* (2021). doi:10.1177/01979183211064829
- 614 18. *Bangladesh Delta Plan 2100*. (2018).
- 615 19. Neu, F. N. & Fünfgeld, H. Political ecologies of resettlement in river deltas. *Geogr. Compass* **16**, (2022).
- 616 20. Szabo, S. *et al.* Population dynamics, delta vulnerability and environmental change:
618 comparison of the Mekong, Ganges–Brahmaputra and Amazon delta regions. *Sustain. Sci.* **11**, 539–554 (2016).
- 619 21. Anderson, D. M., Overpeck, J. T. & Gupta, A. K. Increase in the Asian Southwest Monsoon
621 During the Past Four Centuries. *Science (80-)*. **297**, 596–599 (2002).
- 622 22. Caesar, J., Janes, T., Lindsay, A. & Bhaskaran, B. Temperature and precipitation
623 projections over Bangladesh and the upstream Ganges, Brahmaputra and Meghna
624 systems. *Environ. Sci. Process. Impacts* **17**, 1047–1056 (2015).
- 625 23. Mishra, V. & Lilhare, R. Hydrologic sensitivity of Indian sub-continental river basins to
626 climate change. *Glob. Planet. Change* **139**, 78–96 (2016).
- 627 24. Sandeep, K. *et al.* A multi-proxy lake sediment record of Indian summer monsoon
628 variability during the Holocene in southern India. *Palaeogeogr. Palaeoclimatol.*
629 *Palaeoecol.* **476**, 1–14 (2017).
- 630 25. Sarkar, S. *et al.* Monsoon source shifts during the drying mid-Holocene: Biomarker
631 isotope based evidence from the core 'monsoon zone' (CMZ) of India. *Quat. Sci. Rev.*
632 **123**, 144–157 (2015).
- 633 26. Kudrass, H. R., Hofmann, A., Doose, H., Emeis, K. & Erlenkeuser, H. Modulation and

- amplification of climatic changes in the Northern Hemisphere by the Indian summer monsoon during the past 80 k.y. *Geology* **29**, 63–66 (2001).
27. Banerji, U. S., Arulbalaji, P. & Padmalal, D. Holocene climate variability and Indian Summer Monsoon: An overview. *Holocene* **30**, 744–773 (2020).
28. Wang, Y. *et al.* Abrupt mid-Holocene decline in the Indian Summer Monsoon caused by tropical Indian Ocean cooling. *Clim. Dyn.* **55**, 1961–1977 (2020).
29. Misra, P., Tandon, S. K. & Sinha, R. Holocene climate records from lake sediments in India: Assessment of coherence across climate zones. *Earth-Science Rev.* **190**, 370–397 (2019).
30. Zhao, C. *et al.* Paleoclimate Significance of Reconstructed Rainfall Isotope Changes in Asian Monsoon Region. *Geophys. Res. Lett.* **48**, 1–13 (2021).
31. IPCC. *Climate Change 2014: Synthesis Report. Contribution of Working Groups I, II and III to the Fifth Assessment Report of the Intergovernmental Panel on Climate Change [Core Writing Team, R.K. Pachauri and L.A. Meyer (eds.)]*. (IPCC, 2014).
32. IPCC. *Climate Change 2022: Impacts, Adaptation, and Vulnerability. Contribution of Working Group II to the Sixth Assessment Report of the Intergovernmental Panel on Climate Change [H.-O. Pörtner, D.C. Roberts, M. Tignor, E.S. Poloczanska, K. Mintenbeck, A. Aleg. (Cambridge University Press, 2022)]*.
33. Higgins, S. A., Overeem, I., Rogers, K. G. & Kalina, E. A. River linking in India: Downstream impacts on water discharge and suspended sediment transport to deltas. *Elementa* **6**, (2018).
34. Lutz, A. F., Immerzeel, W. W., Shrestha, A. B. & Bierkens, M. F. P. Consistent increase in

- 656 High Asia's runoff due to increasing glacier melt and precipitation. *Nat. Clim. Chang.* **4**,
657 587–592 (2014).
- 658 35. Milliman, J. D. & Syvitski, J. P. M. Geomorphic / Tectonic Control of Sediment Discharge
659 to the Ocean : The Importance of Small Mountainous Rivers. *J. Geol.* **100**, 525–544
660 (1992).
- 661 36. Milliman, J. D. & Meade, R. H. World-wide Delivery of River Sediment to the Oceans. *J.*
662 *Geol.* **91**, 1–21 (1983).
- 663 37. Rahman, M. *et al.* Recent sediment flux to the Ganges-Brahmaputra-Meghna delta
664 system. *Sci. Total Environ.* **643**, 1054–1064 (2018).
- 665 38. Darby, S. E. *et al.* A first look at the influence of anthropogenic climate change on the
666 future delivery of fluvial sediment to the Ganges–Brahmaputra–Meghna delta. *Environ.*
667 *Sci. Process. Impacts* **17**, 1587–1600 (2015).
- 668 39. Dunn, F. E. *et al.* Projections of historical and 21st century fluvial sediment delivery to the
669 Ganges-Brahmaputra-Meghna, Mahanadi, and Volta deltas. *Sci. Total Environ.* **642**, 105–
670 116 (2018).
- 671 40. Tessler, Z. D., Vörösmarty, C. J., Overeem, I. & Syvitski, J. P. M. A model of water and
672 sediment balance as determinants of relative sea level rise in contemporary and future
673 deltas. *Geomorphology* **305**, 209–220 (2018).
- 674 41. Syvitski, J. *et al.* Earth's sediment cycle during the Anthropocene. *Nat. Rev. Earth Environ.*
675 **3**, 179–196 (2022).
- 676 42. Wang, H. *et al.* Stepwise decreases of the Huanghe (Yellow River) sediment load (1950–
677 2005): Impacts of climate change and human activities. *Glob. Planet. Change* **57**, 331–

- 678 354 (2007).
- 679 43. Miao, C., Ni, J., Borthwick, A. G. L. & Yang, L. A preliminary estimate of human and
680 natural contributions to the changes in water discharge and sediment load in the Yellow
681 River. *Glob. Planet. Change* **76**, 196–205 (2011).
- 682 44. Romans, B. W., Castelltort, S., Covault, J. A., Fildani, A. & Walsh, J. P. Environmental
683 signal propagation in sedimentary systems across timescales. *Earth-Science Rev.* **153**, 7–
684 29 (2016).
- 685 45. D’Haen, K., Verstraeten, G. & Degryse, P. Fingerprinting historical fluvial sediment fluxes.
686 *Prog. Phys. Geogr.* **36**, 154–186 (2012).
- 687 46. Goodbred Jr., S. L. & Kuehl, S. A. Holocene and modern sediment budgets for the
688 Ganges-Brahmaputra river system: Evidence for highstand dispersal to flood-plain, shelf,
689 and deep-sea depocenters. *Geology* **27**, 559–562 (1999).
- 690 47. Goodbred Jr., S. L. & Kuehl, S. A. Enormous Ganges-Brahmaputra sediment discharge
691 during strengthened early Holocene monsoon. *Geology* **28**, 1083–1086 (2000).
- 692 48. Akter, J., Sarker, M. H., Popescu, I. & Roelvink, D. Evolution of the Bengal Delta and Its
693 Prevailing Processes. *J. Coast. Res.* **321**, 1212–1226 (2016).
- 694 49. Garzanti, E. et al. Mineralogical and chemical variability of fluvial sediments 1. Bedload
695 sand (Ganga-Brahmaputra, Bangladesh). *Earth Planet. Sci. Lett.* **299**, 368–381 (2010).
- 696 50. Hay, W. W. Detrital sediment fluxes from continents to oceans. *Chem. Geol.* **145**, 287–
697 323 (1998).
- 698 51. Syvitski, J. P. M. & Saito, Y. Morphodynamics of deltas under the influence of humans.
699 *Glob. Planet. Change* **57**, 261–282 (2007).

- 700 52. Sinha, R., Singh, S., Mishra, K. & Swarnkar, S. Channel morphodynamics and sediment
701 budget of the Lower Ganga River using a hydro-geomorphological approach. *Earth Surf.
702 Process. Landforms* 0–2 (2022). doi:10.1002/esp.5325
- 703 53. Oppenheimer, M. et al. Sea Level Rise and Implications for Low-Lying Islands, Coasts and
704 Communities. in *IPCC Special Report on the Ocean and Cryosphere in a Changing Climate*
705 (eds. Pörtner, H.-O. et al.) 321–445 (Cambridge University Press, 2019).
706 doi:<https://doi.org/10.1017/9781009157964.006>.
- 707 54. Kuehl, S. A., Hariu, T. M. & Moore, W. S. Shelf sedimentation off the Ganges-
708 Brahmaputra river system: Evidence for sediment bypassing to the Bengal fan. *Geology*
709 **17**, 1132–1135 (1989).
- 710 55. Rogers, K. G., Goodbred, S. L. & Khan, S. R. Shelf-to-canyon connections: Transport-
711 related morphology and mass balance at the shallow-headed, rapidly aggrading Swatch
712 of No Ground (Bay of Bengal). *Mar. Geol.* **369**, 288–299 (2015).
- 713 56. Weber, M. E., Wiedicke, M. H., Kudrass, H. R., Hübscher, C. & Erlenkeuser, H. Active
714 growth of the Bengal Fan during sea-level rise and highstand. *Geology* **25**, 315–318
715 (1997).
- 716 57. Kottke, B. et al. Acoustic facies and depositional processes in the upper submarine
717 canyon Swatch of No Ground (Bay of Bengal). *Deep. Res. Part II Top. Stud. Oceanogr.* **50**,
718 979–1001 (2003).
- 719 58. Fournier, L. et al. The Bengal fan: External controls on the Holocene Active Channel
720 turbidite activity. *The Holocene* **7**, 900–913 (2017).
- 721 59. Bendixen, M., Best, J., Hackney, C. & Iversen, L. L. Time is running out for sand. *Nature*

- 722 **571**, 29–31 (2019).
- 723 60. Hackney, C. R. *et al.* River bank instability from unsustainable sand mining in the lower
724 Mekong River. *Nat. Sustain.* **3**, 217–225 (2020).
- 725 61. Best, J. Anthropogenic stresses on the world's big rivers. *Nat. Geosci.* **12**, 7–21 (2019).
- 726 62. Goodbred Jr., S. L. *et al.* Piecing together the Ganges-Brahmaputra-Meghna river delta:
727 Use of sediment provenance to reconstruct the history and interaction of multiple fluvial
728 systems during Holocene delta evolution. *Bull. Geol. Soc. Am.* **126**, 1495–1510 (2014).
- 729 63. Singh, S. K., Rai, S. K. & Krishnaswami, S. Sr and Nd isotopes in River sediments from the
730 Ganga basin: Sediment provenance and spatial variability in physical erosion. *J. Geophys.
731 Res. Earth Surf.* **113**, 1–18 (2008).
- 732 64. Singh, S. K. & France-Lanord, C. Tracing the distribution of erosion in the Brahmaputra
733 watershed from isotopic compositions of stream sediments. *Earth Planet. Sci. Lett.* **202**,
734 645–662 (2002).
- 735 65. Islam, M. R., Begum, S. F., Yamaguchi, Y. & Ogawa, K. The Ganges and Brahmaputra rivers
736 in Bangladesh: basin denudation and sedimentation. *Hydrol. Process.* **13**, 2907–2923
737 (1999).
- 738 66. Lupker, M. *et al.* A Rouse-based method to integrate the chemical composition of river
739 sediments: Application to the Ganga basin. *J. Geophys. Res. Earth Surf.* **116**, 1–24 (2011).
- 740 67. Cecil, C. B., Edgar, N. T., Dulong, F. T. & Neuzil, S. G. Concepts, Models, and Examples of
741 Climatic Controls on Sedimentation: Introduction. in *Climate Controls on Stratigraphy* 5–
742 8 (SEPM (Society for Sedimentary Geology), 2003).
- 743 doi:<https://doi.org/10.2110/pec.03.77.0005>

- 744 68. Kääb, A., Berthier, E., Nuth, C., Gardelle, J. & Arnaud, Y. Contrasting patterns of early
745 twenty-first-century glacier mass change in the Himalayas. *Nature* **488**, 495–498 (2012).
- 746 69. Sinha, R. Kosi: Rising Waters, Dynamic Channels and Human Disasters. *Econ. Polit. Wkly.*
747 **43**, 42–46 (2008).
- 748 70. Gibling, M. R., Tandon, S. K., Sinha, R. & Jain, M. Discontinuity-bounded alluvial
749 sequences of the southern Gangetic plains, India: Aggradation and degradation in
750 response to monsoonal strength. *J. Sediment. Res.* **75**, 369–385 (2005).
- 751 71. Goodbred, S. L. Response of the Ganges dispersal system to climate change: a source-to-
752 sink view since the last interstadia. *Sediment. Geol.* **162**, 83–104 (2003).
- 753 72. Williams, M. A. J. & Clarke, M. F. Late Quaternary environments in north-central India.
754 *Nature* **308**, 633–635 (1984).
- 755 73. Simpson, G. & Castelltort, S. Model shows that rivers transmit high-frequency climate
756 cycles to the sedimentary record. *Geology* **40**, 1131–1134 (2012).
- 757 74. Clift, P. D. *et al.* Holocene erosion of the Lesser Himalaya triggered by intensified summer
758 monsoon. *Geology* **36**, 79–82 (2008).
- 759 75. Sarkar, M. H. & Thorne, C. R. Morphological Response of the Brahmaputra–Padma–
760 Lower Meghna River System to the Assam Earthquake of 1950. in *Braided Rivers* (eds.
761 Jarvis, I., Sambrook Smith, G. H., Best, J. L., Bristow, C. S. & Petts, G. E.) 289–310
762 (Blackwell Publishing Ltd., 2009). doi:<https://doi.org/10.1002/9781444304374.ch14>
- 763 76. Lahiri, S. K. & Sinha, R. Tectonic controls on the morphodynamics of the Brahmaputra
764 River system in the upper Assam valley, India. *Geomorphology* **169–170**, 74–85 (2012).
- 765 77. Kettner, A. J. & Syvitski, J. P. M. HydroTrend v.3.0: A climate-driven hydrological

- 766 transport model that simulates discharge and sediment load leaving a river system.
- 767 *Comput. Geosci.* **34**, 1170–1183 (2008).
- 768 78. Allison, M. A. Historical changes in the Ganges-Brahmaputra delta front. *J. Coast. Res.* **14**,
- 769 1269–1275 (1998).
- 770 79. Brammer, H. Bangladesh's dynamic coastal regions and sea-level rise. *Clim. Risk Manag.*
- 771 **1**, 51–62 (2014).
- 772 80. Sarwar, M. G. M. & Woodroffe, C. D. Rates of shoreline change along the coast of
- 773 Bangladesh. *J. Coast. Conserv.* **17**, 515–526 (2013).
- 774 81. Dunn, F. E. & Minderhoud, P. S. J. Sedimentation strategies provide effective but limited
- 775 mitigation of relative sea-level rise in the Mekong delta. *Commun. Earth Environ.* **3**,
- 776 (2022).
- 777 82. Smajgl, A. *et al.* Responding to rising sea levels in the Mekong Delta. *Nat. Clim. Chang.* **5**,
- 778 167–174 (2015).
- 779 83. Rogers, K. G. & Overeem, I. Doomed to drown? Sediment dynamics in the human-
- 780 controlled floodplains of the active Bengal Delta. *Elementa* **5**, (2017).
- 781 84. Paprocki, K. All That Is Solid Melts into the Bay: Anticipatory Ruination and Climate
- 782 Change Adaptation. *Antipode* **51**, 295–315 (2019).
- 783 85. Auerbach, L. W. *et al.* Flood risk of natural and embanked landscapes on the Ganges–
- 784 Brahmaputra tidal delta plain. *Nat. Clim. Chang.* **5**, 153–157 (2015).
- 785 86. Pethick, J. & Orford, J. D. Rapid rise in effective sea-level in southwest Bangladesh: Its
- 786 causes and contemporary rates. *Glob. Planet. Change* **111**, 237–245 (2013).
- 787 87. van Maren, D. S. *et al.* Tidal amplification and river capture in response to land

- 788 reclamation in the Ganges-Brahmaputra delta. *Catena* **220**, (2023).
- 789 88. Rahman, M. M. *et al.* Sustainability of the coastal zone of the Ganges-Brahmaputra-
- 790 Meghna delta under climatic and anthropogenic stresses. *Sci. Total Environ.* **829**, 154547
- 791 (2022).
- 792 89. Barbour, E. J. *et al.* The unequal distribution of water risks and adaptation benefits in
- 793 coastal Bangladesh. *Nat. Sustain.* **5**, 294–302 (2022).
- 794 90. Bomer, E. J., Wilson, C. A., Hale, R. P., Hossain, A. N. M. & Rahman, F. M. A. Surface
- 795 elevation and sedimentation dynamics in the Ganges-Brahmaputra tidal delta plain,
- 796 Bangladesh: Evidence for mangrove adaptation to human-induced tidal amplification.
- 797 *Catena* **187**, 104312 (2020).
- 798 91. Akter, J., Roelvink, D. & van der Wegen, M. Process-based modeling deriving a long-term
- 799 sediment budget for the Ganges-Brahmaputra-Meghna Delta, Bangladesh. *Estuar. Coast.*
- 800 *Shelf Sci.* **260**, 107509 (2021).
- 801 92. Paszkowski, A., Goodbred, S., Borgomeo, E., Khan, M. S. A. & Hall, J. W. Geomorphic
- 802 change in the Ganges–Brahmaputra–Meghna delta. *Nat. Rev. Earth Environ.* **2021** 1–18
- 803 (2021). doi:10.1038/s43017-021-00213-4
- 804 93. Rampini, C. Hydropower and Sino-Indian Hydropolitics Along the Yarlung-Tsangpo-
- 805 Brahmaputra. in *The Political Economy of Hydropower in Southwest China and Beyond*
- 806 (eds. Rousseau, J. & Habich-Sobiegalla, S.) 235–254 (Palgrave Macmillan, Cham, 2021).
- 807 doi:10.1007/978-3-030-59361-2_12
- 808 94. Jiang, H. *et al.* Framing the Brahmaputra River hydropower development: different
- 809 concerns in riparian and international media reporting. *Water Policy* **19**, 496–512 (2017).

- 810 95. Grumbine, R. E. & Pandit, M. K. Threats from India's Himalaya dams. *Science (80-.)*. **339**,
811 36–37 (2013).
- 812 96. Menon, M. & Kohli, K. From impact assessment to clearance manufacture. *Econ. Polit.*
813 *Wkly.* **44**, 20–23 (2009).
- 814 97. Singh, J. S. Sustainable development of the Indian Himalayan region: Linking ecological
815 and economic concerns. *Curr. Sci.* **90**, 784–788 (2006).
- 816 98. Agrawal, R. Polluters Rewarded. *countercurrents.org* (2008). Available at:
817 <https://countercurrents.org/agrawal040308.htm>.
- 818 99. Arora, N. & Ghoshal, D. India plans dam on Brahmaputra to offset Chinese construction
819 upstream. *Reuters* (2020). Available at: <https://www.reuters.com/article/us-india-china->
820 hydropower-idUKKBN28B4NN.
- 821 100. Li, D. *et al.* Exceptional increases in fluvial sediment fluxes in a warmer and wetter High
822 Mountain Asia. *Science (80-.)*. **374**, 599–603 (2021).
- 823 101. Dewan, C. *Misreading the Bengal Delta - Climate Change, Development, and Livelihoods*
824 *in Coastal Bangladesh*. (University of Washington Press, 2022).
- 825 102. Wilson, C. A. & Goodbred Jr., S. L. Construction and Maintenance of the Ganges-
826 Brahmaputra-Meghna Delta: Linking Process, Morphology, and Stratigraphy. *Ann. Rev.*
827 *Mar. Sci.* **7**, 67–88 (2015).
- 828 103. Grimaud, J. L. *et al.* Flexural deformation controls on Late Quaternary sediment dispersal
829 in the Garo-Rajmahal Gap, NW Bengal Basin. *Basin Res.* **32**, 1252–1270 (2020).
- 830 104. Pickering, J. L. *et al.* Terrace formation in the upper Bengal basin since the Middle
831 Pleistocene: Brahmaputra fan delta construction during multiple highstands. *Basin Res.*

- 832 **30**, 550–567 (2018).
- 833 105. Pickering, J. L. *et al.* Late Quaternary sedimentary record and Holocene channel avulsions
834 of the Jamuna and Old Brahmaputra River valleys in the upper Bengal delta plain.
- 835 *Geomorphology* **227**, 123–136 (2014).
- 836 106. Sincavage, R., Goodbred, S. & Pickering, J. Holocene Brahmaputra River path selection
837 and variable sediment bypass as indicators of fluctuating hydrologic and climate
838 conditions in Sylhet Basin , Bangladesh. 302–320 (2018). doi:10.1111/bre.12254
- 839 107. Ayers, J. C. *et al.* Sources of salinity and arsenic in groundwater in southwest Bangladesh.
840 *Geochem. Trans.* **17**, 1–22 (2016).
- 841 108. Ahmed, M. K., Islam, S., Rahman, M. S., Haque, M. R. & Islam, M. M. Heavy Metals in
842 Water , Sediment and Some Fishes of Buriganga River, Bangladesh. *Int. J. Environ. Res.* **4**,
843 321–332 (2010).
- 844 109. BADC (Bangladesh Agricultural Development Corporation). Deep Tubewell II Project:
845 Final Reports. (1992).
- 846 110. Khan, S. R. & Islam, B. Holocene stratigraphy of the lower Ganges-Brahmaputra river
847 delta in Bangladesh. *Front. Earth Sci. China* **2**, 393–399 (2008).
- 848 111. Michels, K. H., Kudrass, H. R., Hübscher, C., Suckow, A. & Wiedicke, M. The submarine
849 delta of the Ganges-Brahmaputra: Cyclone-dominated sedimentation patterns. *Mar.*
850 *Geol.* **149**, 133–154 (1998).
- 851 112. Palamenghi, L., Schwenk, T., Spiess, V. & Kudrass, H. R. Seismostratigraphic analysis with
852 centennial to decadal time resolution of the sediment sink in the Ganges-Brahmaputra
853 subaqueous delta. *Cont. Shelf Res.* **31**, 712–730 (2011).

- 854 113. Sarkar, A. *et al.* Evolution of Ganges-Brahmaputra western delta plain: Clues from
855 sedimentology and carbon isotopes. *Quat. Sci. Rev.* **28**, 2564–2581 (2009).
- 856 114. Pickering, J. L. *et al.* Impact of glacial-lake paleofloods on valley development since glacial
857 termination II : A conundrum of hydrology and scale for the lowstand Brahmaputra-
858 Jamuna paleovalley system. *GSA Bull.* **131**, 58–70 (2018).
- 859 115. Shamsudduha, M., Uddin, A., Saunders, J. A. & Lee, M. K. Quaternary stratigraphy,
860 sediment characteristics and geochemistry of arsenic-contaminated alluvial aquifers in
861 the Ganges-Brahmaputra floodplain in central Bangladesh. *J. Contam. Hydrol.* **99**, 112–
862 136 (2008).
- 863 116. Pate, R. D., Goodbred, S. L. & Khan, S. R. Delta Double-Stack: Juxtaposed Holocene and
864 Pleistocene Sequences from the Bengal Basin, Bangladesh. *Sediment. Rec.* **7**, 4–9 (2009).
- 865 117. DPHE-JICA (Department of Public Health Engineering and Japanese International
866 Cooperation Agency). *Development of deep aquifer database and preliminary deep*
867 *aquifer map. Final Report.* (2006).
- 868 118. (JICA), J. I. C. A. Geology and Stone material, Part 1: Geology. in **6**, 133 (Japan
869 International Cooperation Agency, 1976).
- 870 119. Ghosal, U., Sikdar, P. K. & McArthur, J. M. Palaeosol Control of Arsenic Pollution: The
871 Bengal Basin in West Bengal, India. *Groundwater* **53**, 588–599 (2015).
- 872 120. Hait, A. K. *et al.* New dates of Pleisto-Holocene subcrop samples from South Bengal,
873 India. *Indian J. Earth Sci.* **23**, 79–82 (1996).
- 874 121. Hoque, M. A., McArthur, J. M. & Sikdar, P. K. The palaeosol model of arsenic pollution of
875 groundwater tested along a 32km traverse across West Bengal, India. *Sci. Total Environ.*

- 876 **431**, 157–165 (2012).
- 877 122. Hoque, M. A., McArthur, J. M. & Sikdar, P. K. Sources of low-arsenic groundwater in the
878 Bengal Basin: investigating the influence of the last glacial maximum palaeosol using a
879 115-km traverse across Bangladesh. *Hydrogeol. J.* **22**, 1535–1547 (2014).
- 880 123. Grall, C. *et al.* A base-level stratigraphic approach to determining Holocene subsidence of
881 the Ganges–Meghna–Brahmaputra Delta plain. *Earth Planet. Sci. Lett.* **499**, 23–36 (2018).
- 882 124. Sincavage, R. S., Paola, C. & Goodbred, S. L. Coupling Mass Extraction and Downstream
883 Fining With Fluvial Facies Changes Across the Sylhet Basin of the Ganges-Brahmaputra-
884 Meghna Delta. *J. Geophys. Res. Earth Surf.* **124**, 400–413 (2019).
- 885 125. Reitz, M. D. *et al.* Effects of tectonic deformation and sea level on river path selection:
886 Theory and application to the Ganges-Brahmaputra-Meghna River Delta. *J. Geophys. Res.
887 Earth Surf.* **120**, 671–689 (2015).
- 888 126. Lambeck, K., Rouby, H., Purcell, A., Sun, Y. & Sambridge, M. Sea level and global ice
889 volumes from the Last Glacial Maximum to the Holocene. *Proc. Natl. Acad. Sci. U. S. A.*
890 **111**, 15296–15303 (2014).
- 891 127. Kuehl, S. A., Levy, B. M., Moore, W. S. & Allison, M. A. Subaqueous delta of the Ganges-
892 Brahmaputra river system. *Mar. Geol.* **144**, 81–96 (1997).
- 893 128. Garzanti, E. *et al.* Provenance of Bengal Shelf Sediments: 2. Petrology and Geochemistry
894 of Sand. *Minerals* **9**, 642 (2019).
- 895 129. Lupker, M., France-Lanord, C., Galy, V., Lavé, J. & Kudrass, H. Increasing chemical
896 weathering in the Himalayan system since the Last Glacial Maximum. *Earth Planet. Sci.
897 Lett.* **365**, 243–252 (2013).

- 898 130. Stanley, D. J. & Hait, A. K. Holocene depositional patterns, neotectonics and Sundarban
899 mangroves in the western Ganges-Brahmaputra delta. *J. Coast. Res.* **16**, 26–39 (2000).
- 900 131. Pate, R. D. Multiple-proxy records of delta evolution and dispersal system behavior:
901 fluvial and coastal borehole evidence from the Bengal Basin, Bangladesh. (Vanderbilt
902 University, 2008).
- 903 132. Ullah, M. S. Provenance analysis and depositional system of the Late Quaternary
904 sediment from the Ganges-Brahmaputra delta, Bangladesh: Application of strontium
905 geochemistry. (Vanderbilt University, 2010).
- 906 133. Woodruff, J. D., Irish, J. L. & Camargo, S. J. Coastal flooding by tropical cyclones and sea-
907 level rise. *Nature* **504**, 44–52 (2013).
- 908 134. Kay, S. *et al.* Modelling the increased frequency of extreme sea levels in the Ganges–
909 Brahmaputra–Meghna delta due to sea level rise and other effects of climate change.
910 *Environ. Sci. Process. Impacts* **17**, 1311–1322 (2015).
- 911 135. Darby, S. E., Dunn, F. E., Nicholls, R. J., Rahman, M. & Riddy, L. A first look at the influence
912 of anthropogenic climate change on the future delivery of fluvial sediment to the
913 Ganges–Brahmaputra–Meghna delta. *Environ. Sci. Process. Impacts* **17**, 1587–1600
914 (2015).
- 915 136. Clemens, S. C. *et al.* Remote and local drivers of Pleistocene South Asian summer
916 monsoon precipitation : A test for future predictions. *Sci. Adv.* **7**, eabg3848 (2021).
- 917

918 **ACKNOWLEDGEMENTS**

919 This work was supported in part by U.S. National Science Foundation grants OISE-0968354 to
920 M.S.S., S.L.G., and C.P., RISE-1342946 to S.L.G., OCE-1600319 to S.L.G., J.C.A., J.M.G., OCE-
921 1600258 to C.A.W., BCS- 1716909 to C.A.W., K.G.R., and J.M.G., and U.S. Office of Naval
922 Research grant N00014-11-1-0683 to S.L.G., J.C.A., M.S.S. and J.M.G. The authors also thank
923 contributions from Rachel L. Bain and Thomas R. Hartzog and field support from the
924 Department of Geology, University of Dhaka and Nazrul Islam Bachchu of Pugmark Tours and
925 Travels. The manuscript was considerably improved based on feedback from reviewer Andrew
926 Large, an anonymous reviewer, and editors Rebecca Neely and Melissa Plail.

927

928 **AUTHOR CONTRIBUTION STATEMENT**

929 All authors contributed to the project's intellectual development and success. S.L.G., C.P., and
930 M.S.S. designed the original study and K.M.A., S.H.A., M.R.K., and M.M.R. supported in-country
931 study design and local research contexts. J.L.R., J.L.P., R.S.S., M.S.H., C.A.W., D.R.M., J.-L.G.,
932 C.J.G., K.G.R., M.D., R.P.H., M.G.M., and L.A.W. conducted the field sampling and lab analyses.
933 J.L.R., S.L.G., J.L.P., R.S.S., C.A.W., B.N.C., and J.M.G. developed and analyzed the dataset. J.L.R.
934 and S.L.G. wrote the manuscript with contributions from J.L.P., R.S.S., J.C.A., C.A.W., C.P.,
935 M.S.S., C.J.G., K.G.R., E.A.C., and R.P.H. All authors reviewed and commented on the
936 manuscript.

937

938 **COMPETING INTERESTS STATEMENT**

939 The authors declare no competing interests.

940

941 **Figures and Tables**

942

943 **Figure 1. Map of Bengal basin and the Ganges-Brahmaputra River delta in South Asia showing**

944 **the study area and and drilling/sampling and data locations.** The delta and lower Ganges and

945 Brahmaputra rivers are located in Bangladesh and West Bengal, India. The Holocene delta

946 developed on an incised Pleistocene surface and the boundary of Holocene deposits is shown

947 by the black dashed line. The subaqueous portion of the Holocene delta is located on the shelf

948 and bordered by the Swatch of No Ground canyon and Bay of Bengal to the south. Over 450

949 boreholes from this study are denoted by the dark and light gray--filled circles ^{123,131,132}, with

950 the light gray circles demarking Transect G cores shown in Figure S1. Core and acoustic-flection

951 data from other studies used to define the thickness and extent of Holocene delta deposits are

952 shown by white-filled circles ^{108–113,115,117,119–121}. The border of Bangladesh is outlined in pink,

953 and the pink-shaded region represents the higher-risk coastal zone based on the model domain

954 used in Akter et al. (2021) ⁹¹. World Ocean Base layer is from Esri, GEBCO, NOAA NGDC, HERE,

955 Garmin, and other contributors; the world countries shapefile is from Esri, Garmin

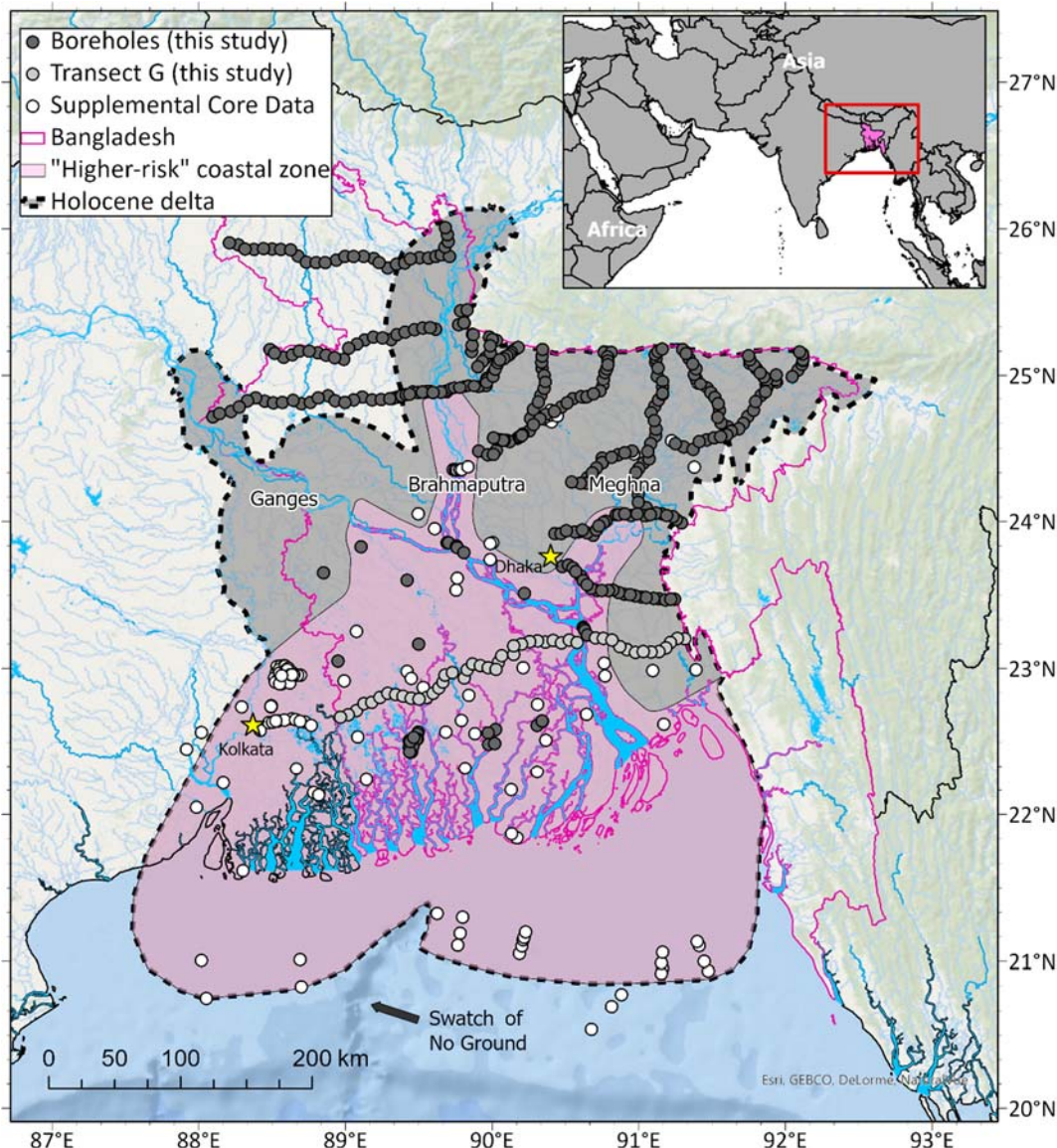
956 International, Inc., and the U.S. Central Intelligence Agency (The World Factbook); and the

957 hydrology shapefiles (World Water Bodies and World Linear Water) are from Esri and Garmin

958 International, Inc..

959

960



961

962

963

964

965 **Table 1.** Average mass storage rates and grain size distributions for deposits stored on the

966 Ganges-Brahmaputra delta over the last 12 kyr. Highest rates of sediment delivery and storage

967 in the delta occur between 10–8 ka and correspond with a sandier sediment load.

Years	Silt and clay (Mt/yr) (<62.5 µm)	Very fine-fine sand (Mt/yr) (62.5-250 µm)	Medium-coarse sand (Mt/yr) (250-1000 µm)
6-0 ka *	389	294	162
8-6 ka *	425	519	309
10-8 ka	505	824	671
12-10 ka	171	277	371

* Offshore mass distributed with 75% of offshore material contained in the 6-0 ka unit and 25% of offshore material contained in the 8-6 ka unit.

968

969

970

971

972

973

974

975

976

977

978

979

980

981

982 **Table 2.** Average mass storage rates and percent contribution for each river system throughout
 983 the Holocene. The Brahmaputra is the main contributor of sediment in the early-mid Holocene
 984 (12–6 ka), while the Ganges delivers most of the sediment over the last 6 kyr. Storage rate data
 985 are plotted in Figure 2C.

6–0 ka

Source	Storage Rate (Mt/yr)	Percent Contribution
Ganges	426	50.4%
Brahmaputra	377	44.7%
Mixed G+B	7	0.8%
Other	35	4.1%
Total	845	

8–6 ka

Source	Storage Rate (Mt/yr)	Percent Contribution
Ganges	308	24.6%
Brahmaputra	726	58.0%
Mixed G+B	17	1.3%
Other	202	16.1%
Total	1253	

10–8 ka

Source	Storage Rate (Mt/yr)	Percent Contribution
Ganges	413	20.7%
Brahmaputra	1119	55.9%
Mixed G+B	128	6.4%
Other	340	17.0%
Total	2001	

12–10 ka

Source	Storage Rate (Mt/yr)	Percent Contribution
Ganges	116	14.2%
Brahmaputra	512	62.6%
Mixed G+B	16	2.0%
Other	174	21.2%
Total	818	

986

987

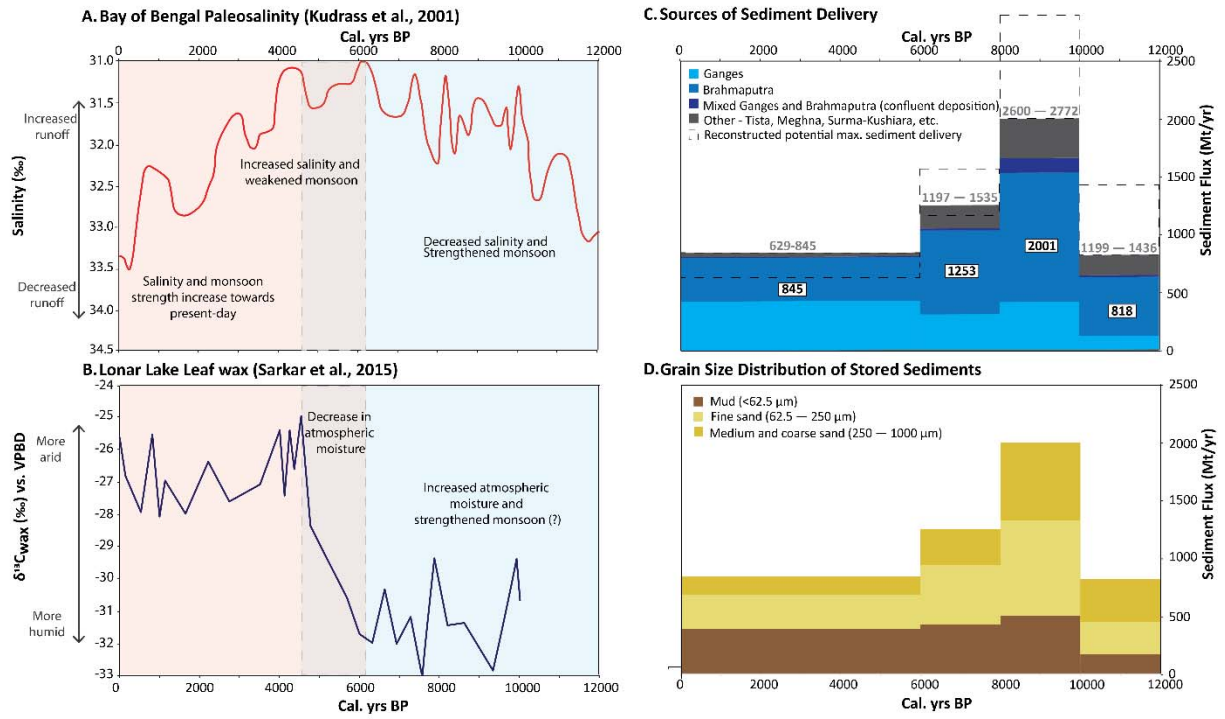
988

989

990

991 **Figure 2. Holocene variability in sediment mass and caliber corresponds with changes in**
992 **paleosalinity and atmospheric moisture.** A) A paleosalinity record from sediment cores
993 collected in the northern Bay of Bengal²⁶ provides a proxy record for an enhanced early
994 Holocene monsoon, when runoff and river discharge increased and lowered salinity of the
995 surface mixed layer. Salinities decrease after 6 ka under weakening monsoon precipitation and
996 reduced (but still large) river discharge. B) Terrestrial records of leaf-wax stable carbon
997 isotopes from lacustrine sediments in Lonar Lake, central India²⁵ provide evidence for
998 increased atmospheric moisture during the Holocene Climatic Optimum (~9-5 ka), with sharply
999 decreasing moisture levels with monsoon weakening after ~6 ka. C-D) Sediment mass and
1000 caliber varies over the Holocene. In the early Holocene, most sediment was deposited by the
1001 Brahmaputra River, followed by the Ganges. For the last 6 kyr, the two rivers have deposited a
1002 roughly equivalent mass of sediment on the delta but with few deposits reflecting any mixing
1003 between them. Other tributary sources have locally contributed sediment to the delta, but the
1004 amount is comparatively minor. Observed sediment delivery rates over the Holocene are
1005 denoted in white boxes and the reconstruction of the maximum potential sediment load based
1006 on bypassing estimates are shown in gray text within the dashed boxes.

1007

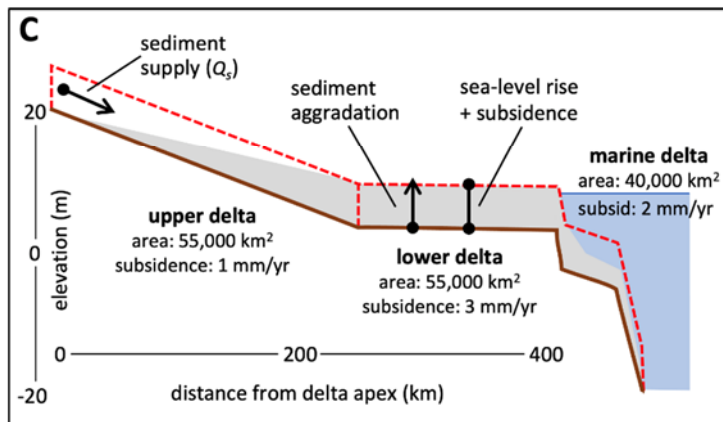


1008

1009

1010 **Figure 3. Modern, Holocene, and future mass-balance calculations comparing rates of**
 1011 **sediment delivery against the mass required to offset sea-level rise and subsidence. (A)**
 1012 Summary of the mass-balance scenarios, showing input values for sediment supply and sea-
 1013 level rise and the calculated outputs for Δ Mass and $f_{(supply)}$. Calculations of required mass for
 1014 each scenario can be found in Table S4. (B) An explanation of the calculated terms, the
 1015 conditions for each Δ Mass case, and the data sources are provided along with (C) a schematic
 1016 diagram of the mass-balance model for the delta. The Holocene: 10-8 ka scenario considers
 1017 only the high sediment demand case, as the whole delta aggraded in response to rapid sea-
 1018 level rise during this period.

A Scenario	Supply (Mt/yr)	S.L. Rise (mm/yr)	Δ Mass (Mt/yr)			$f_{(supply)}$
			low	medium	high	
20 th century: typical Q _s	1,100 ^a	2.5 ^f	367	232	88	27%
20 th century: low Q _s	700 ^a	2.5 ^f	-33	-168	-313	-19%
Holocene: 6-0 ka	845 ^b	0.5 ^g	419	344	283	69%
Holocene: 8-6 ka	1,253 ^b	4.8 ^g	384	220	29	21%
Holocene: 10-8 ka	2,001 ^b	12.5 ^g	--	--	792	66% (high)
2050 climate only ^a	1,349 ^c	5.6 ^f	139	-89	-361	-6%
2100 climate only ^a	1,624 ^c	8.5 ^f	-32	-347	-739	-18%
River-linking (partial) ^b	866 ^d	8.5 ^f	-790	-1,105	-1,497	-56%
River-linking (all) ^b	600 ^d	8.5 ^f	-1,056	-1,371	-1,763	-70%
2100 full impacts ^c	85 ^e	8.5 ^f	-1,571	-1,886	-2,278	-96%



B **CALCULATED TERMS:**
 Δ Mass = $Mass_{(supply)} - Mass_{(required)}$ where:

- $Mass_{(required)} = SUM[Area_{(sub-region)} \times RSLR_{(sub-region)}]$ for each sub-region upper, lower, and marine
- $RSLR_{(sub-reg)} = Eustatic SLR + Subsidence_{(sub-reg)}$

 $f_{(supply)}$ = fraction of sediment supply for which delta is in excess or deficit (medium sediment case only)

△-MASS CASES:

- **low sediment demand** = the lower delta aggrades at the pace of RSLR, with the upper and marine deltas aggrading at 0.5 x RSLR – allows some non-deposition in higher portions of upper delta and some likely coastal erosion and ravinement of shelf.
- **medium sediment demand** = the lower delta and marine area receive full aggradation to offset RSLR and protect the coast, and the upper delta accretes at 0.5 x RSLR – a reasonable scenario to maintain shoreline stability and limit lower-delta flooding.
- **high sediment demand** = the entire delta requires full aggradation to offset RSLR – less likely scenario requiring all areas to receive maximum sediment.

• **excess supply**, **slight deficit**, **large deficit**

SUPPLY and SEA-LEVEL RISE SCENARIOS:

- ^a Rahman et al. (2018), *Sci. Tot. Enviro.*, **643**:1054.
- ^b this study
- ^c Darby et al. (2015), *Enviro. Science*, **17**:1587.
- ^d Higgins et al. (2018), *Elementa*, **6**:20.
- ^e Dunn et al. (2019), *Enviro. Res. Letters*, **14**:084034.
- ^f IPCC (2019), Cambridge Press, SROCC Chapter 4.
- ^g Lambeck et al. (2014), *PNAS*, **111**(43):15296.

1022

1023

1024

1025

1026

1027

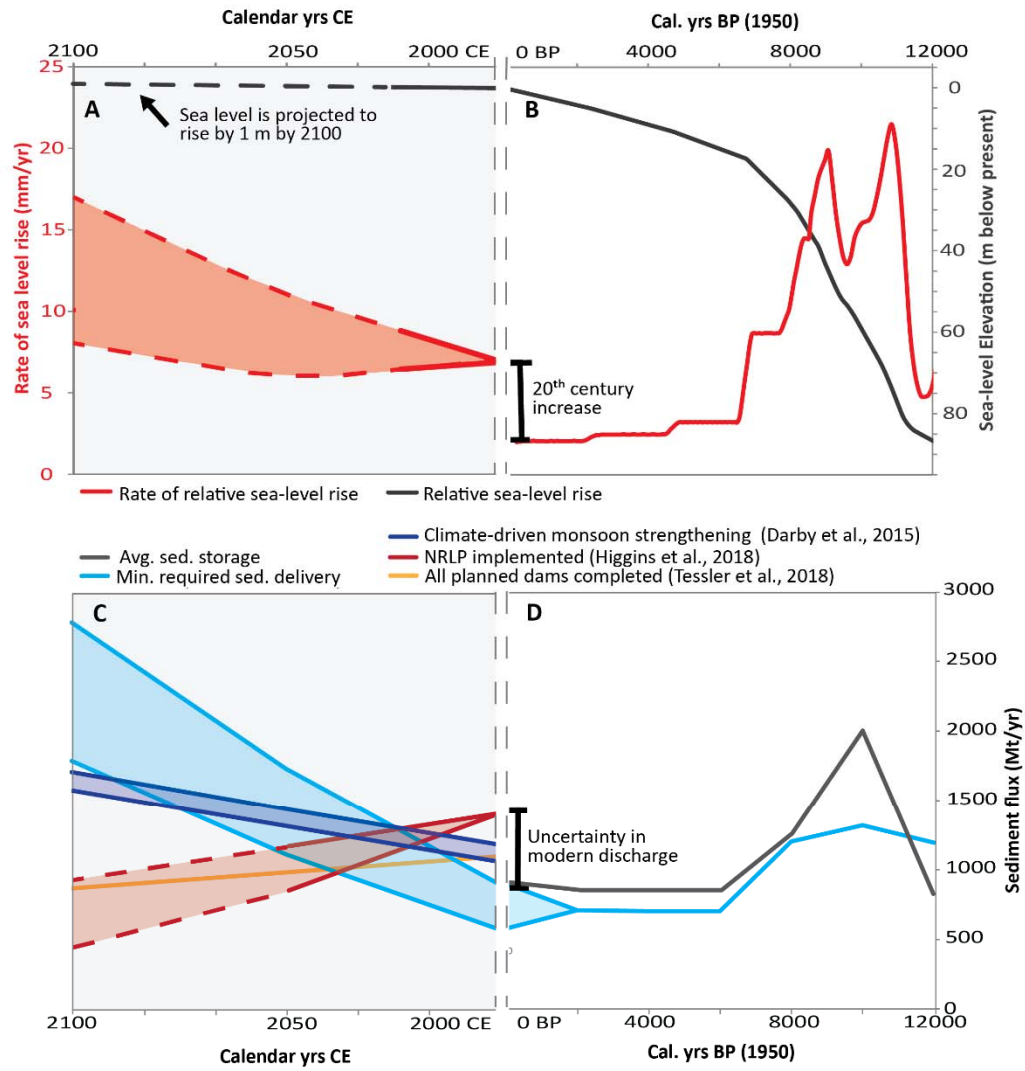
1028

1029

1030

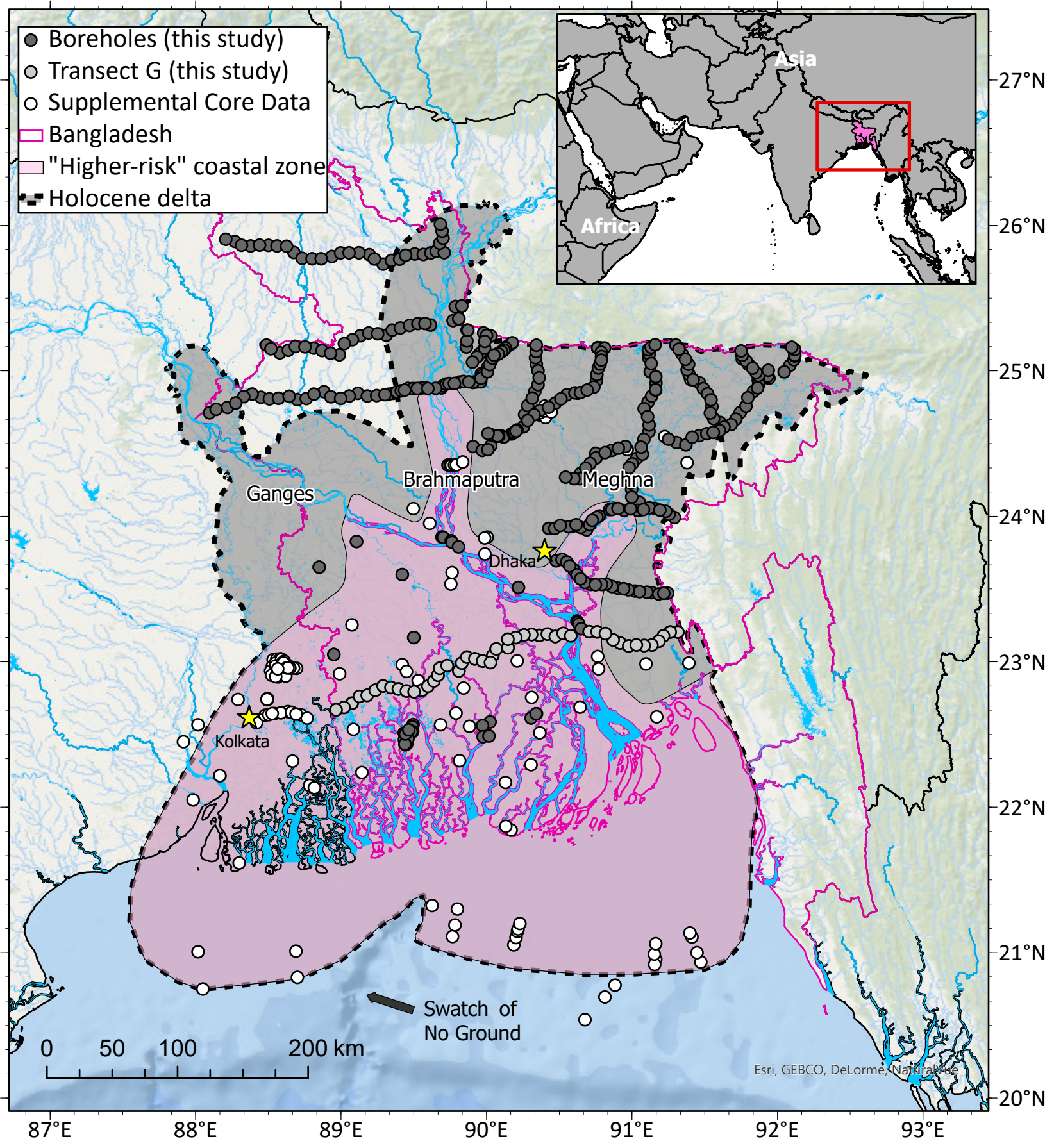
1031

1032 **Figure 4. Holocene and predicted future changes in sea level and sediment delivery to the**
1033 **Ganges-Brahmaputra.** A) Comparison of future changes in sea level (shown relative to 1992 CE)
1034 ¹³³ to B) Holocene changes in global sea level (shown relative to EGM96) ¹²⁶. Local sea level (not
1035 shown) ¹³⁴ and relative sea level is expected to rise by ~1 m by 2100 (blue line, panel A). C) In
1036 the future, predicted changes in monsoon strength ¹³⁵ and river damming with the National
1037 River Linking Project (NRLP) ^{33,40} indicate that sediment fluxes reaching the delta may increase
1038 or be reduced. Minimum required sediment delivery is calculated using the whole delta area
1039 (Table S4), so less sediment delivery may still sustain the at-risk portions of the delta against
1040 rising sea level. D) The rate of sediment storage on the delta exceeded the necessary sediment
1041 required to keep pace with sea level between 10–8 ka, and for the last 8 ka, whole-delta
1042 storage rates have closely matched or exceeded sediment requirements **contributing to**
1043 **progradation of the delta.** Ultimately, changes in sediment delivery to the delta are likely to
1044 occur from river damming ^{33,40}, sand mining ^{59,60}, strengthening monsoon ¹³⁶, and
1045 anthropogenic climate change ^{135,136}.



1046

1047



Years	Silt and clay (Mt/yr) (<62.5 µm)	Very fine-fine sand (Mt/yr) (62.5-250 µm)	Medium-coarse sand (Mt/yr) (250-1000 µm)
6-0 ka *	389	294	162
8-6 ka *	425	519	309
10-8 ka	505	824	671
12-10 ka	171	277	371

* Offshore mass distributed with 75% of offshore material contained in the 6-0 ka unit and 25% of offshore material contained in the 8-6 ka unit.

6–0 ka

Source	Storage Rate (Mt/yr)	Percent Contribution
Ganges	426	50.4%
Brahmaputra	377	44.7%
Mixed G+B	7	0.8%
Other	35	4.1%
Total	845	

8–6 ka

Source	Storage Rate (Mt/yr)	Percent Contribution
Ganges	308	24.6%
Brahmaputra	726	58.0%
Mixed G+B	17	1.3%
Other	202	16.1%
Total	1253	

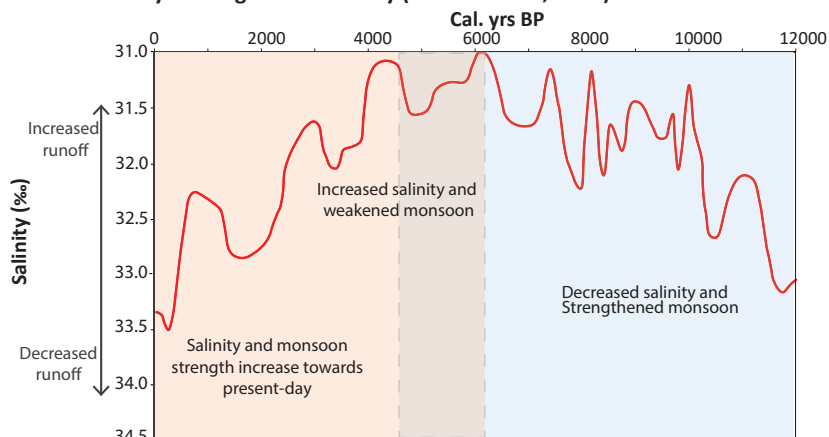
10–8 ka

Source	Storage Rate (Mt/yr)	Percent Contribution
Ganges	413	20.7%
Brahmaputra	1119	55.9%
Mixed G+B	128	6.4%
Other	340	17.0%
Total	2001	

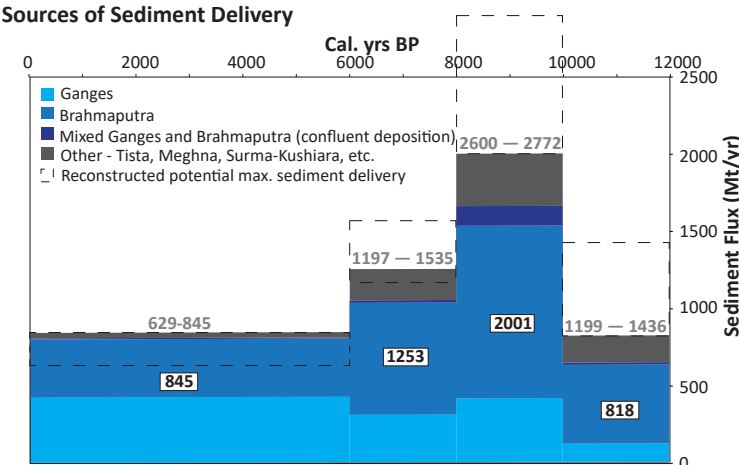
12–10 ka

Source	Storage Rate (Mt/yr)	Percent Contribution
Ganges	116	14.2%
Brahmaputra	512	62.6%
Mixed G+B	16	2.0%
Other	174	21.2%
Total	818	

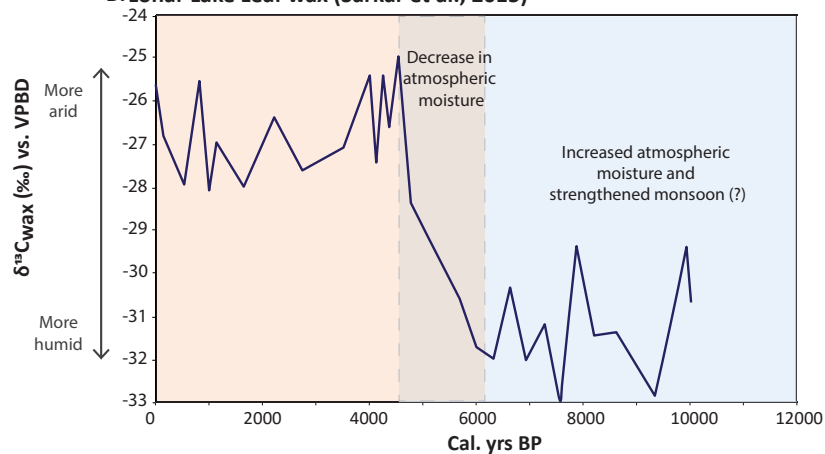
A. Bay of Bengal Paleosalinity (Kudrass et al., 2001)



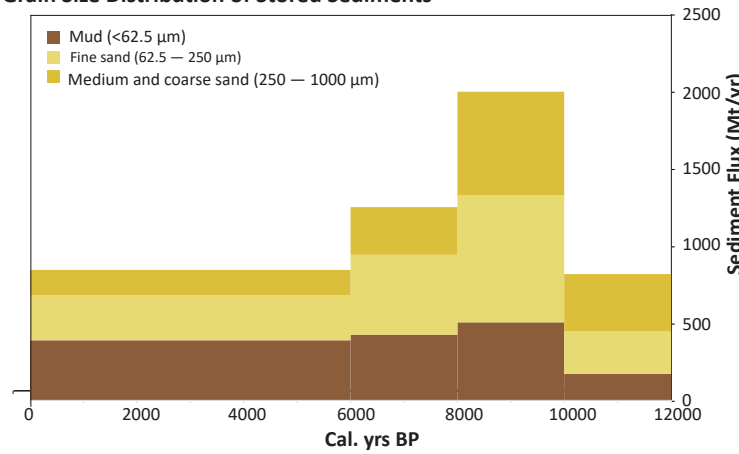
C. Sources of Sediment Delivery



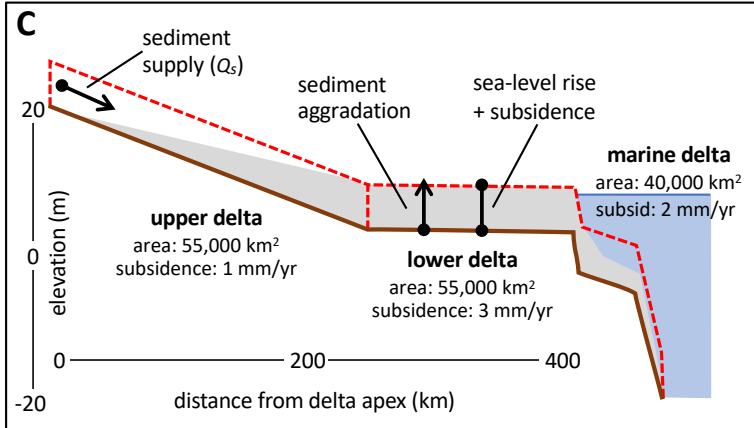
B. Lonar Lake Leaf wax (Sarkar et al., 2015)



D. Grain Size Distribution of Stored Sediments



A Scenario	Supply (Mt/yr)	S.L. Rise (mm/yr)	Δ Mass (Mt/yr)			$f_{(supply)}$ medium
			low	medium	high	
20 th century: typical Q_s	1,100 ^a	2.5 ^f	367	232	88	27%
20 th century: low Q_s	700 ^a	2.5 ^f	-33	-168	-313	-19%
Holocene: 6-0 ka	845 ^b	0.5 ^g	419	344	283	69%
Holocene: 8-6 ka	1,253 ^b	4.8 ^g	384	220	29	21%
Holocene: 10-8 ka	2,001 ^b	12.5 ^g	--	--	792	66% (high)
2050 climate only ^a	1,349 ^c	5.6 ^f	139	-89	-361	-6%
2100 climate only ^a	1,624 ^c	8.5 ^f	-32	-347	-739	-18%
River-linking (partial) ^b	866 ^d	8.5 ^f	-790	-1,105	-1,497	-56%
River-linking (all) ^b	600 ^d	8.5 ^f	-1,056	-1,371	-1,763	-70%
2100 full impacts ^c	85 ^e	8.5 ^f	-1,571	-1,886	-2,278	-96%



B

CALCULATED TERMS:

▲ **Mass** = $Mass_{(supply)} - Mass_{(required)}$ where:

- $Mass_{(required)} = \text{SUM}[\text{Area}_{(\text{sub-region})} \times RSLR_{(\text{sub-region})}]$ for each sub-region upper, lower, and marine
- $RSLR_{(\text{sub-reg})} = \text{Eustatic SLR} + \text{Subsidence}_{(\text{sub-reg})}$

$f_{(supply)}$ = fraction of sediment supply for which delta is in excess or deficit (medium sediment case only)

△-MASS CASES:

- **low sediment demand** = the lower delta aggrades at the pace of RSLR, with the upper and marine deltas aggrading at 0.5 x RSLR – allows some non-deposition in higher portions of upper delta and some likely coastal erosion and ravinement of shelf.
- **medium sediment demand** = the lower delta and marine area receive full aggradation to offset RSLR and protect the coast, and the upper delta accretes at 0.5 x RSLR – a reasonable scenario to maintain shoreline stability and limit lower-delta flooding.
- **high sediment demand** = the entire delta requires full aggradation to offset RSLR – less likely scenario requiring all areas to receive maximum sediment.

• █ = excess supply, █ = slight deficit, █ = large deficit

SUPPLY and SEA-LEVEL RISE SCENARIOS:

^a Rahman et al. (2018), *Sci. Tot. Enviro.*, **643**:1054.
^b this study
^c Darby et al. (2015), *Enviro. Science*, **17**:1587.
^d Higgins et al. (2018), *Elementa*, **6**:20.
^e Dunn et al. (2019), *Enviro. Res. Letters*, **14**:084034.
^f IPCC (2019), Cambridge Press, SROCC Chapter 4.
^g Lambeck et al. (2014), *PNAS*, **111**(43):15296.

